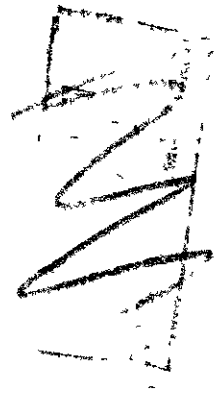


MINISTRY OF SUPPLY

AERONAUTICAL RESEARCH COUNCIL
CURRENT PAPERS



Flight Tests on the Youngman-Baynes High-Lift Experimental Aircraft

By

D. Lean, B.Sc., A.F.R.Ae.S.

Crown Copyright Reserved

LONDON: HIS MAJESTY'S STATIONERY OFFICE

1952

Price 10s. 6d. net.

ROYAL AERONAUTICAL ESTABLISHMENT
LIBRARY

C.P. No.65

Report No. Aero. 2390

August, 1950

ROYAL AIRCRAFT ESTABLISHMENT

Flight Tests on the Youngman-Baynes High-Lift
Experimental Aircraft

by

D. Lean, B.Sc., A.F.R.Ae.S.

SUMMARY

Flight tests on the Youngman-Baynes Experimental High-Lift aircraft have shown that an increment of maximum lift coefficient of 1.32 can be obtained on an unswept wing with a low drag section, whose basic maximum lift coefficient is 1.28. It is estimated that an increment of maximum lift coefficient of 0.2 has been lost due to the adverse effect of wing-fuselage interference.

Adequate lateral control in all conditions of flight is provided by ailerons inset in the full span flap.

The profile drag coefficient increment at full flap is 0.07 for a lift coefficient increment of 1.14, at a wing incidence of 10 degrees.

The changes in longitudinal trim due to the flaps are small and easily controlled and the effect of ground on longitudinal trim is considered negligible, since there is no difficulty in landing with flaps down.

The structure of the wing-flap-aileron arrangement is adequately stiff in torsion, and the aileron reversal speed is estimated to be nearly 300 knots.

LIST OF CONTENTS

	<u>Page</u>
1 Introduction	4
2 Description of Aircraft	4
3 Test Equipment	5
4 Flight Test Programme and Technique	6
4.1 Stalling Behaviour, and measurement of Maximum Lift Coefficients	6
4.2 Partial Glides	7
4.3 Trim Curves	8
4.4 Ground Effect on Trim	9
4.5 Lateral Control and Response	9
4.6 Rate of Climb Measurements	10
5 Results and Discussion	10
5.1 Maximum Lift Coefficients, and Stalling Behaviour	10
5.2 Wing-Fuselage Interference Effects	13
5.3 Lift and Drag Measurements	14
5.4 Trim Changes due to Flaps and Engine Power	17
5.5 Ground Effect on Pitching Moments	19
5.6 Lateral Control Characteristics	20
5.6.1 Rates of Rotation	20
5.6.2 Response	22
5.6.3 Aileron Reversal Speed	23
5.7 General Handling Qualities	24
6 Conclusions	25
References	25

LIST OF TABLES

Tables I to VIII	- See Text
Table IX	Aerodynamic Data - Youngman-Baynes Experimental Aircraft

LIST OF ILLUSTRATIONS

	<u>Fig.</u>
3-View G.A. of Youngman-Baynes Experimental Aircraft	1
Front and Side views of Youngman-Baynes Experimental Aircraft	2
Rear Views, showing flaps extended	3

LIST OF ILLUSTRATIONS (contd.)

	<u>Fig.</u>
Relation between main and auxiliary flap deflections	4
Wing sections at root and tip (flaps down)	5
Total Position Error Corrections	6
Growth of Stalled Area with Reduction in Speed - Flaps Up	7
Growth of Stalled Area with Reduction in Speed - Flaps Down	8
C_L - α Curves from Partial Glide Measurements	9
C_D - α Curves from Partial Glide Measurements	10
Comparison between Model and Full Scale Lift Curves	11
Comparison between Estimated and Measured Lift Increments due to Flaps	12
Variation of Total and Profile Drag Coefficients with C_L	13
Variation of Profile Drag Coefficient with Incidence	14
Lift and Profile Drag increments due to Flaps	15
Variation of C_D/C_L with Lift Coefficient	16
Variation of Angle of Glide with Airspeed	17
Variation of Datum Attitude with Lift Coefficient	18
Variation of Elevator Angle to Trim with Lift Coefficient	19
Variation of $p_b/2V$, $r_b/2V$ with Lift Coefficient	20
Time History of Typical Rudder-fixed Aileron Roll, Flaps Down	21
Variation of $p_b/2V$ with Speed Margin over the Stall	22
Variation of Aileron Power with Airspeed	23
Time to Apply a Given Angle of Bank	24
Prediction of Aileron Reversal Speed	25
Climb Performance at Ground Level and 5000 feet	26

1 Introduction

In order to operate highly loaded aircraft from restricted spaces, such as forward airfields, or the decks of aircraft carriers, the chosen wing-flap systems must be capable of producing high maximum lift coefficients. In addition, if high performance in top speed or range is to be maintained, it is essential that the brackets and links of the flap operating system should be contained, as far as possible, within the wing profile. A large double slotted flap which, when retracted, fairs neatly into the profile of an unswept low drag section wing, of thickness/chord ratio 0.13, with only one small excrescence, has been designed by Mr. R.T. Youngman. The lift, drag and pitching moment characteristics of this flap arrangement have been investigated by means of low speed tunnel tests¹. The first tests were made on a rectangular wing alone, to fix the optimum flap settings and to investigate the rolling power of the proposed aileron arrangement. From this information a 1/5 scale model of the aircraft designed for the full-scale flight tests (described in this report) was constructed and tested in the No.2 11½ ft x 8½ ft tunnel. This investigation of the fuselage and tail plane effects on lift and longitudinal control and stability is reported in Reference 2.

The present report is concerned with the flight tests of the full scale aircraft, and deals mainly with the low speed characteristics of the wing-flap arrangement. Where possible, a comparison is made between the flight results and those of the two series of tunnel tests.

2 Description of Aircraft

A 3-view general arrangement drawing of the aircraft is given in Fig.1, and four photographic views of the aircraft are shown in Figs.2 and 3. It will be seen that the aircraft bears a strong resemblance to the Proctor IV civil aircraft, though, in fact, only the undercarriage and rudder, plus a few minor items, are standard Proctor IV parts.

The aircraft is a single-engined, two-seater, low wing monoplane, of conventional layout, fitted with a Gipsy Queen 32 engine of 250 H.P. driving a 7 ft 6 inches diameter constant speed propeller. The normal take-off weight was 3700 lb, with the C.G. at 36.6% of the mean chord.

The wing is a low drag section of the N.A.C.A. 65 - 2 series modified to an elliptical nose section over the outboard part of the span (see Reference 1), with the further modification of a drooped nose over that part of the span inboard of the undercarriage. This latter modification is apparent in the head-on view in Fig.2.

The forward, fixed part of the wing is of wooden construction, while the rear 50%, including the flaps and ailerons, is constructed of light alloy. The main flap is of 96% span and 50% chord. Incorporated in this flap is the auxiliary rear flap, of 25% chord, covering the central 54% of the span, while the outboard portion of the main flap carries the Frise ailerons, of 25% total chord. The aileron appears to be of larger chord than the auxiliary flap in the photographs, because of the large shroud which covers the leading edge of the flap. These photographs were taken after the central portion of the auxiliary flap had been removed (see Section 5.1).

The flaps are suspended from the fixed part of the wing and from the fuselage, by a system of links operated by a total of six screw jacks. These jacks are rotated by a shaft located aft of the front

spar and driven by an electric motor on the centre line of the aircraft. The flaps can move rearwards and downwards so that the main flap, carrying the aileron with it, is depressed 15 degrees relative to the wing while the auxiliary flap travels a further 30 degrees and lies at 45 degrees relative to the wing. The total rearward extension of the flaps amounts to 24% of the wing chord. The relation between the angles of the main and auxiliary flap relative to the wing is shown in Fig.4. The "half flap" setting was arbitrarily chosen to give about one-third of the flap travel.

When the flaps are down, a slot is formed between the leading edge of the main flap, and the fixed main plane, and a second slot is formed between the leading edge of the rear flap and the inboard portion of the main flap. The relation between the main flap and the ailerons is unchanged when the flaps move, so that the ailerons droop 15 degrees when the flaps are fully down.

The sizes and shapes of these slots are shown in Fig.5. The size of the rear slot shown as 1.8%, was originally 3.0%, and was modified to the size shown as a result of the stalling speed and maximum lift measurements discussed in section 5.1 below.

The remainder of the aircraft is conventional and needs little comment. The fuselage is about 1 ft longer than that of the standard Proctor, and the elevator area is about 100% greater. The rather large tail volume coefficient of 0.7 was chosen to ensure positive static longitudinal stability up to the stall, and the extra elevator area as a safeguard against possibly large trim changes due to lowering the flaps. The tail plane setting is adjustable on the ground over the range -1 degree to +5 degrees relative to the wing chord, but the -1 degree setting was used throughout the tests.

It was originally intended to fit sealed pressure balance ailerons to this aircraft (Reference 1), and although the 2-dimensional model tests showed these to give adequate rolling power, it was considered wiser to build the full scale aircraft with the more conventional Frise ailerons.

The remaining aerodynamic data for the aircraft is given in Table IX at the end of the report.

3 Test Equipment

For the airspeed measurements, the aircraft was fitted with a 100 ft suspended static head, operated manually by the observer, and a venturi pitot mounted on a short strut under the starboard wing. The standard aircraft system pitot-static head was fitted on a similar strut under the port wing.

An automatic observer was installed for the recording of the following quantities:-

- 1 Airspeed indicator reading - either on the standard aircraft system, or on the venturi pitot - suspended static system.
- 2 Altitude - measured either by the aircraft static or the suspended static system.
- 3 Engine speed.

- 4 Attitude of the aircraft in pitch and roll, measured by an electrically driven gyro.
- 5 Acceleration, in a direction roughly normal to the flight path, using a remote indicating accelerometer of the Barnes type.
- 6 Elevator angle, using a desynn transmitter connected to the elevator operating lever in the tail.
- 7 Angle of main flap relative to the wing, at the inboard and outboard ends, using desynn transmitters, for both wings.
- 8 Angle of auxiliary flap relative to the main flap, for both wings, using desynn transmitters.

Records of the readings of the above instruments were obtained by means of an electrically driven Bell and Howell 35 mm cine camera. In addition, for the lateral control investigations, records were obtained on a 4-channel continuous trace recorder of the following quantities.

- 1 Aileron angles relative to the main flap, port and starboard using desynn transmitters.
- 2 Rate of roll about the longitudinal axis of the aircraft, using an electrically-driven spring-constrained gyro.
- 3 Rate of yaw about the vertical axis of the aircraft, also using an electrically-driven spring-constrained gyro.

Records from this instrument, and those from the normal automatic observer were synchronised by using a common timing system which marked each record at half-second intervals.

4 Flight Test Programme and Technique

4.1 Stalling Behaviour, and Measurement of Maximum Lift Coefficients

The initial investigation of the stalling behaviour was made before the installation of the full flight test instrumentation equipment. The object was to obtain a quick measurement of the maximum lift coefficients and to study the conditions of airflow over the upper wing surface at and near the stalling incidence. Measurements of stalling speed were made by visual observation with the flaps up, half down, and fully down, with the engine throttled back.

The characteristics of the airflow at and near the stall were studied by means of wool tufts attached to the upper wing surface. Twenty groups of tufts were attached to each wing, each group consisting of 4 strands at various heights up to about 10 inches above the wing surface. Only direct visual observation of the tufts was made. The airspeed was reduced in steps, down to the stalling speed, and at each steady speed the flow pattern was sketched in, from observation of the behaviour of the tufts.

When the full recording equipment was installed, the measurements of stalling speed were repeated in more detail, including the effect of power. Continuous records of the airspeed indicator (operating on the venturi pitot-trailing static system), normal acceleration, and attitude in pitch, plus a measurement of the rate of descent from readings of the altimeter, provided the information necessary for an exact evaluation of the maximum lift coefficient.

Each record was obtained by first trimming for steady flight conditions, with the engine at the required setting, at a speed about 10 m.p.h. above the indicated minimum speed. The stick was then eased slowly back so that the speed decreased at a rate of less than $\frac{1}{2}$ m.p.h. per second, with the automatic observer switched on. Recording was continued until the speed was building up again during the recovery.

When the engine was throttled back, with the flaps fully down, the speed fell rapidly almost to the stalling speed, and had to be increased to the required steady value before a suitable recording could be started.

It was intended originally that the observer should indicate the exact point on the record at which the stall occurred, by switching on a lamp in the automatic observer instrument panel, but it was found that a more reliable indication was obtained from the readings of the accelerometer and the pitch indicator, both of which changed rapidly at the stall. The reading of the A.S.I. continued to fall for a short time after the stall, often by as much as 2 m.p.h. and is therefore not a reliable means, by itself, for the measurement of stalling speed.

From the first few records, a reasonable estimate of the stalling incidence was obtained, and the accuracy of the acceleration measurements was then improved by setting the instrument so that the recording axis was approximately at right angles to the flight path at the stall. The wing lift was then equal to the weight (allowing for fuel consumption) multiplied by the accelerometer reading in g-units, with only a small correction for mis-alignment of the accelerometer axis.

A correction had to be applied to the reading of the airspeed indicator to compensate for the effect of the rate of change of static pressure at the suspended static head. With 100 ft of comparatively small-bore tubing between the static head and the indicator, the pressure in the static side of the instrument lagged behind the actual pressure at the static head, and with a positive rate of descent, the instrument gave a high reading. This correction was proportional to the rate of descent and often amounted to over 1 m.p.h.

When measuring the maximum lift coefficients in the power-on condition, the contribution of the slipstream and the airscrew thrust to the total lift coefficient was estimated by the method given in Reference 3. Propeller thrust coefficients were estimated by means of the charts of Ref.4. By subtracting this contribution from the gross lift coefficient, the lift coefficient attributable to the wing and flaps alone was obtained. Throughout this report, reference to maximum lift coefficient, power-on, implies that the above correction has been applied.

A total of 46 stalls was recorded, covering the three flap settings, with power off and power on, and included a study of the effects of various changes to the flaps and upper wing root surface, as described in Section 5.1.

4.2 Partial Glides

The object of these tests was to produce curves showing the variation of lift and total drag coefficients with incidence, for direct comparison with the results of the model tests.

Steady, straight glides were made, with the aircraft in the required condition as regards speed and flap position, and with the engine speed adjusted so that the propeller was giving zero thrust.

This latter condition was satisfied by setting the propeller speed control for maximum R.P.M. so that the propeller was in fully fine pitch, and then, knowing the blade setting, and using the charts of Reference 4, the R.P.M. was adjusted on the throttle to the value corresponding to zero thrust coefficient at the known true airspeed.

The steady glides were maintained for about 30 seconds, and the rate of descent recorded by means of the altimeter and a stopwatch. During this interval, 4 short records were obtained on the automatic observer, so as to obtain mean values of the indicated airspeed, attitude in pitch, normal acceleration and elevator angle (required for the production of trim curves).

From the measured aneroid rate of descent and the mean equivalent airspeed, the angle of glide could be estimated, knowing the air temperature and relative pressure at the mean altitude of each glide. Results were always corrected to standard atmospheric conditions. Given the angle of glide and the attitude of the aircraft, the angle of incidence could be obtained.

Lift and drag coefficients were obtained from a knowledge of the instantaneous aircraft weight, angle of glide and equivalent airspeed. Airspeeds were measured on the standard aircraft system, to avoid having to correct the aircraft drag for the drag of the suspended static head. Equivalent airspeeds were obtained from a knowledge of the total position error correction, measured by a separate flight test. Position error curves are shown in Fig.6.

The drag coefficient was corrected for any residual thrust or drag which the airscrew might have provided, due to incorrect setting of the R.P.M.

The measurements were made at as wide a range of speeds as possible, with flaps down and half down, and up to nearly 130 knots, flaps up. The tests were repeated, following the modifications to the flaps, etc., discussed in the next section.

It was found that very calm air conditions were essential if consistent results were to be obtained. Up - or down - currents were natural sources of error, and general "bumpiness" prevented the pilot from maintaining either a steady speed or a constant attitude in pitch. The scatter of the points on the final curves arose mainly from the difficulty of estimating the incidence, since even a slight correction to the speed necessitated a comparatively large change in attitude.

4.3 Trim Curves

The magnitude of the changes in longitudinal trim produced by changes in speed, flap angle and engine power was investigated by obtaining records of the elevator angle to trim with various combinations of the above three parameters.

The majority of the data for the engine-off trim curves were obtained from the records of the partial glide tests. Elevator angles to trim at the stall were obtained from the records of the stalling tests.

Separate flight tests were necessary to obtain the corresponding curves with power on, with the engine set for maximum continuous cruising power. These tests were done with the suspended static head in use, so as to obtain the total position error correction at the same time.

Since information was required only on the pitching moment changes due to the flaps at various lift coefficients, with power off and power on, no measurements were made of the stick forces to trim, nor was any attempt made to determine the static margin by repeating the tests at a different C.G. position. Movement of the C.G. would, in any case, have been very difficult, since the aircraft was already 100 lb over the design maximum weight.

The elevator trimmer was, in all cases, set neutral, so no correction to the elevator angle to trim was required on this account.

4.4 Ground Effect on Trim

Information was required on the effect of the proximity of the ground on the elevator angle to trim with flaps up and down. Since it was impossible to obtain trim curves in the normal way with the aircraft flying sufficiently close to the ground for the ground effect to be apparent, an alternative, though admittedly less satisfactory method had to be used.

A series of landing tests was made, with the flaps in each of the three positions. The approach speed and engine condition were chosen so that at the end of the check the aircraft was in the 3-point attitude, and touched down without floating. Continuous automatic observer records were obtained of airspeed indicator reading, attitude and elevator angle.

The main difficulty in assessing the effect of ground arose from a lack of knowledge of the exact condition of the aircraft at the end of the check, and, in particular, from the difficulty of estimating the lift coefficient at this point. Readings of the airspeed indicator were considered to be unreliable, due to the (unknown) effect of ground on the position error correction. This effect is likely to be large, with an under-wing position for the pitot-static head.

It has therefore been assumed that just before touch-down, the aircraft was in trimmed, level flight. The wing incidence was obtained from the record of the aircraft datum attitude, and the elevator angle to trim at this incidence in free flight was obtained from the appropriate trim curve (section 4.3). The difference between this elevator angle, and the actual elevator angle used at touch-down then gave a measure of the effect of the ground on pitching moment at a constant incidence.

4.5 Lateral Control and Response

Automatic observer recordings were obtained of the rolling and yawing behaviour of the aircraft following sudden application of the ailerons, the rudder being held fixed. The tests were made with the flaps at each of the three normal settings (i.e. up, half-down and fully down), at a range of speeds from approximately 1.15 times the stalling speed up to the limiting speed of the aircraft. The engine was set to give maximum continuous cruising power in all cases. The pilot was helped in applying a constant aileron angle by providing him with a series of wire loops of different lengths, attached to each side of the cockpit, so that by attaching the chosen loop to the stick, the ailerons could be moved rapidly to the desired position and held fixed.

The rates of roll and yaw about body axes were measured by electrically-driven spring constrained gyros, recording on a continuous trace 4-channel recorder, which also bore records of the positions of

the two ailerons. These rates of rotation were transformed to corresponding rates about wind axes, using incidence measurements obtained from the results of the partial glide tests.

Unfortunately, the rate of yaw instrument responded not only to pure yawing motion but also to the inevitable rate of change of direction of the flight path following the application of bank. Measurements of adverse yawing are therefore underestimated, since this yawing motion is partly counteracted by the tendency of the aircraft to turn in the direction of the bank. It has not been possible to estimate the exact amount of this error, but it is believed to be small since the maximum rates of roll and yaw were attained within 1 or 2 seconds of the start of the manoeuvre.

It would have been possible for the pilot to use the rudder so as to keep the flight path straight during the roll, but this would have had the effect of masking almost completely the adverse yawing motion, to which considerable interest was attached. It was therefore considered better to hold the rudder fixed, in the hope that the important part of the motion would be completed before any appreciable rate of turn developed.

From the structural point of view, the aileron-flap arrangement on this aircraft is of considerable interest. The rolling forces due to the ailerons are applied at the outboard ends of the main flaps, which are therefore subjected to a considerable torsion moment. This might be expected to result in a rather low aileron reversal speed.

Rates of roll (with flaps up) were, therefore, measured at a range of speeds up to 180 knots E.A.S., which was just over the design limiting diving speed of the aircraft. The speed at which the aileron power (defined as rate of roll per unit aileron angle) became zero was then predicted by the method suggested by Refs. 5 and 6 (see section 5.6 below).

An attempt was also made to measure the amount of twist of the main flap arising from the aileron loads during these high speed rolls.

4.6 Rate of Climb Measurements

It was proposed at an early stage in the flight test programme that the maximum lift coefficient of the aircraft should be increased by the addition of split flaps to the existing slotted flaps. For reasons of simplicity, these flaps would have to be fixed in position (i.e. non-retractable) and would therefore cause a loss in rate of climb, even with the normal flaps retracted. It was therefore necessary to measure the rate of climb performance of the aircraft, in order to determine what amount of extra flap, if any, could safely be added.

Rough measurements of the rate of climb were therefore made at a range of airspeeds, with the normal flaps up, and fully down, with the engine giving its maximum climb power. The tests were made at a mean altitude of 5000 feet, and the results corrected to standard sea-level conditions.

As a result of these tests, it was decided not to proceed with this project.

5 Results and Discussion

5.1 Maximum lift coefficients and stalling behaviour

With the aircraft in its original condition, the following mean

values of the maximum lift coefficient were obtained, each value being the mean of at least 5 measurements. The corresponding values obtained from the 3-dimensional model tests are also given, for comparison (Ref.2).

Table I

Flap Position	Flight Test Reynolds Number	Maximum Lift Coefficients	
		Flight Tests (Engine Off)	Model tests, at R.N. = 1.37×10^6 , (Trimmed values)
Flaps down	2.6×10^6	2.41 (14°)	2.50 (13.5°)
Half Flap	3.1×10^6	1.66 (11°)	-
Flaps up	3.6×10^6	1.28 (16°)	1.16 (20.5°)

Note - the figures in brackets are the corresponding stalling incidences, which, in the case of the flight measurements, may be as much as 2 degrees in error.

The measurements of maximum lift coefficient with flaps up and flaps half down do not call for detailed comment. The difference of 0.1 between the model and full scale measurements in the flaps up case is explained partly by the higher Reynolds number of the full scale tests, and partly by the fact that on the full scale aircraft, the inboard portion of the wing was of slightly different section than that used for the model tests. The drooped nose of the section over this portion of the span is apparent in the head-on photograph in Fig.2.

The rather low stalling incidence recorded when the flaps were half down may have been due to the fact that this setting was an arbitrary one, and no effort was made to produce the optimum size or shape of the gaps between the flaps and the wing.

The disappointingly low value of 2.41 for the maximum lift coefficient in the flap-down case called for further investigation. A visual examination of the upper wing surfaces at the root showed that, while there were no obvious features which might disturb the airflow in this region (the general condition of the wing surface being quite good), there were, nevertheless, several minor gaps and irregularities which, together, might have promoted an early breakaway of the flow. This part of the wing was, therefore, faired over as completely as possible by means of strips of doped fabric. The stalling tests were repeated, and, from 7 such tests, a mean maximum lift coefficient of 2.60 was obtained with flaps down and engine off, with a stalling incidence of about 15 degrees. With the flaps up, however, no significant improvement was observed.

Not only was the stalling speed reduced, with flaps down, as a result of this sealing process, but there was also a marked change in stalling behaviour. Whereas previously, the port wing (which accommodated a rather badly fitting hinged door in its leading edge, giving access to the oil tank) usually dropped at the stall, followed by the nose, the stall was now much more violent, but straightforward, with no tendency to drop either wing.

With engine on (1500 R.P.M. in fine pitch) the stall was even more violent, and the mean maximum lift coefficient, from 4 stalls, corrected for the contribution of slip stream lift and airscrew thrust, was 2.62 with a stalling incidence of around 17 degrees. (The effect of the above amount of engine power was to increase the maximum gross lift coefficient by just over 0.2).

The improvement in the upper wing surface therefore produced a gain in maximum lift coefficient of 0.2, with flaps down.

Previously, the airflow over the upper wing surface had been studied by means of wool tufts. Information was obtained on the growth of the stalled region of airflow as the stall was approached. Figs.7 and 8 show pictorially the result of this investigation for the flaps-up and flaps-down cases respectively.

The development of the stall in the flaps-up case exhibited no unusual features, but the corresponding picture for the flaps-down case (left-hand side of Fig.8) suggested that the gap between the auxiliary and main flaps was the origin of a disturbance in the flow over the rear flap. This disturbance appeared at an early stage, and spread forwards and outwards from this region as the speed was reduced.

The size of the gap between the auxiliary and the main flaps was originally 3% of the wing chord on the full scale aircraft, as it was also on the 3-dimensional model. The 2-dimensional model tests, however, (Ref.1), were made with a gap of 1.8% of the wing chord, this having been found to be the optimum size. It was therefore considered possible that the gap on the full scale aircraft was not, in fact, of the optimum size, and the gap was, therefore, reduced to 1.8% of the wing chord (Fig.5).

This reduction in gap size did not, however, have the expected effect on the maximum lift coefficient, although wool tuft observations suggested that the flow had been improved, as can be seen from the right-hand picture of Fig.8. A mean maximum lift coefficient of 2.50 was obtained with flaps down and engine off, and 2.48 with engine on, with stalling incidences of 16 degrees and 19 degrees respectively. Four stalling records were obtained in each case.

To save time, the remaining tests were all made with this modified gap, although it was then realised that the optimum gap size was probably nearer the original 3% than the modified 1.8%.

In a final attempt to increase the maximum lift coefficient, the effect of removing that portion of the auxiliary flaps which extended across the underside of the fuselage was studied. The reasons for expecting an improvement in this direction are discussed in section 5.2. The portion removed covered the central 9% of the wing span (Fig.3).

Time was not available to make as complete an investigation of this modification as had been done for the others but a maximum lift coefficient of 2.44 was indicated with flaps down and engine off, at an approximate stalling incidence of 14 degrees, increasing to 2.66 at 20 degrees with engine on (1500 R.P.M. in fine pitch, as before).

The results of these investigations are summarised in the following table. Although stalling incidences are quoted in this table, the angles may be as much as 2 degrees in error.

Table II

Condition of Aircraft	Engine Off		Engine On	
	C_L max.	Stalling Incidence	C_L max.	Stalling Incidence
Original	2.41	14°	-	-
Upper Wing root surface faired over	2.60	15°	2.62	17°
Ditto, plus reduced flap gap	2.50	16°	2.48	19°
Ditto, plus central cut-out	2.44	14°	2.66	20°

Note - The correction which has been applied to the maximum lift coefficients with engine on amounted normally to just over 0.2.

It is difficult to draw conclusions from these results, regarding the optimum flap arrangement on this aircraft. Nothing was gained by reducing the rear flap gap to 1.8% of the chord, but there might possibly have been a gain when the central portion of the rear flap was removed, if only when the local flow over the wing was improved with the help of the slipstream. Despite the inaccuracies in the measurements of stalling incidence, there appears to be an increase in this quantity in the presence of slipstream.

A maximum lift coefficient of 2.60, with engine off has thus been established for this aircraft, without modification to the flaps, and it is now necessary to determine why this value is 0.25 less than the value which was estimated from the original 2-dimensional model tests (Ref.1).

5.2 Wing-fuselage interference effects

It is apparent from the 3-dimensional model tests of Ref.2 that the addition of the fuselage to the plain wing had a marked effect on the maximum lift coefficient with flaps down, although the effect was very small with flaps up. In fact, the addition of the fuselage reduced the maximum lift coefficient from 2.81 (c.f. the value of 2.85 estimated in Ref.1) to 2.55, untrammed. This loss in C_L max is due entirely to the lower stalling incidence resulting from the addition of the fuselage - in fact, at a given incidence, the lift coefficient is slightly higher with the fuselage in position than without it.

The difference between the estimated maximum lift coefficient and that achieved on the actual aircraft is therefore probably due to the premature break-away of the flow arising from interference between the fuselage and the deflected flaps. Various wing root fillets were tested in the tunnel (Ref.2) and the simple slab-sided fillet finally used was embodied in the full scale aircraft, but it is probable that this was not of the optimum size or shape.

Earlier wind tunnel model tests reported in Refs. 7 and 8 deal with body interference on a high lift wing. Tests were made on a rectangular wing with a double slotted flap in the presence of a fuselage. In the low wing position, it was found that a higher value of C_L max could be obtained if the flaps were not continued under the body. When the flaps were continuous, the root stall started at an incidence of 4 degrees, but if there was a central cut-out, the stall did not start till an incidence of 7 degrees was reached. With this central cut-out, the stalling incidence and the lift curve slope were both increased. On the other hand both the above model tests and later flight tests (Ref. 9) have shown that, with a wing of taper ratio 2.5:1, it is better to continue the flaps underneath the fuselage. It was therefore suggested that the wing on the Youngman-Baynes aircraft, with its low taper ratio of 1.35:1, corresponded most nearly to the untapered case, and it was decided to remove the central portion of the auxiliary flap.

Unfortunately, the tests of this arrangement were inconclusive. There was a loss in lift with engine off and a gain with engine on. Since the tests were done after the flap gap size had been altered, it is possible that had this gap been of the optimum size, a more definite result might have been obtained.

It is concluded that the early root stall is inherent in the almost rectangular planform, low wing, layout. Various schemes have been suggested for improving the root flow conditions, such as a leading edge slat, or a small local extension of the wing surface running forward along the fuselage from the root leading edge. This would be similar to the dorsal extension to the fin fitted to certain aircraft in order to maintain the fin lift curve slope at large angles of yaw. There was, however, no opportunity for testing any such modifications.

To obtain the best results from this flap arrangement, a tapered wing with a mid or high-wing arrangement seems advisable.

5.3 Lift and Drag Measurements

The results of the partial glide tests were converted to measurements of lift and total drag coefficients at a range of wing incidence, for each of the three flap settings, and the resulting lift and drag curves are plotted in Figs. 9 and 10. The end points on the lift curves of Fig. 8 were obtained from the results of the stalling tests, discussed earlier, each point being the mean result of a number of stalling tests, following the various modifications to the flaps that were investigated. The lift coefficients for the "engine-on" stalls have all been corrected for the contribution of slipstream and airscrew thrust to the total lift. It is again emphasized that incidence measurements at the stall are much less reliable than those obtained during the partial glide tests.

In Fig. 11, a comparison is made between the full scale and the model lift curves, the model curves having been corrected to trimmed conditions. It can be seen that the lift curve slope is less on the full scale aircraft, but that the maximum lift coefficient, flaps down, is higher than that obtained from the model tests, because of the higher stalling incidence.

In the following table, the lift increments due to full deflection of the flaps at a wing incidence of 10 degrees above the no-lift angle, flaps up, and at the stalling incidence, are compared for the full scale and the model tests. The lift curve slopes at 10 degrees incidence are also given, with flaps up and down.

Table III

	Full Scale Tests R.N = 2.5 - 6.5 x 10 ⁶	Model Tests(Ref.2) R.N = 1.37 x 10 ⁶	
		Complete Model, Trimmed	Wing Alone
Lift Coefficient Increment due to Flaps, wing incidence = 10°	1.14	1.31	1.42
Increment of Maximum lift coefficient due to Flaps	1.32	1.34	1.65
Lift Curve Slope, C _L /radian, Flaps Up.	3.63	4.24	4.06
Lift Curve Slope, C _L /radian, Flaps Down.	4.40	5.02	4.35

It is of interest to compare the measured increments of lift coefficient due to the flaps with the increments estimated by the method of Young, given in Ref.10. The flaps are treated as 50% chord double slotted flaps over the inboard portion, and as 50% chord single slotted over the outboard portion of the span. The lift increments at a wing incidence of 10 degrees have been estimated for a range of flap angles up to the full deflection, and the results plotted as the full line in Fig.12. The measured results at 10 degrees incidence are marked in as two points (for half flap and full flap deflection) on the dotted line. Also shown are the tunnel value of the lift coefficient increment at 10 degrees incidence, and the full scale increments of maximum lift coefficient at the two flap deflections. The agreement between the estimated and measured increments is considered to be satisfactory.

These increments of lift coefficient due to flaps all refer to a wing of aspect ratio 6.0. The same flap arrangement, on a wing of aspect ratio 10.0, should produce an increment of lift coefficient, at incidences below the stall, some 11% greater than that actually obtained (Ref.10).

The partial glide tests, with flaps down, were repeated, following the alteration to the gap between the main and auxiliary flaps, and the improvement in the condition of the upper wing surface at the root. The results are plotted on the appropriate curves in Figs.9 and 10, where it can be seen that these modifications had no detectable effect on either lift or drag at a given incidence.

Using the faired lift and drag curves in Figs.9 and 10, the curves showing the variation of total drag coefficient with lift coefficient, given in Fig.13 are obtained. The dotted curves in this diagram show the variation, with lift coefficient, of the difference between the total drag coefficient and the ideal induced drag coefficient $C_L^2/\pi A$. The positive slope of these curves indicates the extent of the deviation from ideal elliptic loading. The departure from ideal loading is partly due to the inboard double slotted flap since this produces a larger local lift coefficient than the outboard single slotted flap.

There is a resulting increase in the induced drag and this must be estimated before the profile drag of the flap can be determined:

The induced drag coefficient may be expressed as

$$C_{Di} = C_L^2 / \pi A + K (\Delta C_L)^2$$

where ΔC_L is the extra lift increment provided by the double slotted flap compared with a single slotted flap of the same size, and K is a factor depending on flap geometry. Strictly speaking, the first term in this expression for C_{Di} should be multiplied by a factor $(1 + \tau)$ to account for the non-elliptic loading of the unflapped wing, but in this analysis we are concerned only with the increment of profile drag due to the flaps. The profile drag coefficient is therefore somewhat loosely defined as the total drag coefficient minus the induced drag coefficient as defined above. The factor K is estimated by a method given by Young in Ref.10.

The profile drag coefficient is plotted in Fig.14 as a function of wing incidence for each flap deflection. The increment of profile drag coefficient due to the flaps is almost independent of incidence over the range of incidence used during take-off and landing. Also shown in Fig.14 are similar curves obtained from an analysis of the wind tunnel results, (Ref.2), for the complete model and for the model wing alone. Defining the profile drag coefficient increment as that measured at an incidence of 6 degrees above the no-lift angle, the following values for ΔC_{Do} are obtained.

Table IV

Flap Position	ΔC_{Do} = Profile Drag Coefficient Increment at $\alpha = \alpha_0 + 6^\circ$		
	Flight Test	Complete Model	Model Wing Alone
Half Flap	0.023	-	-
Full Flap	0.071	0.062	0.048

The difference between the profile drag increment on the model wing alone and that measured on the complete aircraft is indicative of the effect of wing-body interference. The ratio of ΔC_{Do} with interference to ΔC_{Do} without interference, from the model tests, is 1.3, while the ratio of the flight test increment to that for the model wing alone is about 1.5. Young, in Ref.10, suggests an average value of 1.4 for this ratio.

The relation between the lift and profile drag increments due to the flaps is illustrated in Fig.15. The profile drag increment is defined above, and the lift coefficient increment is measured at 10 degrees above the no-lift incidence, flaps up. Comparing this diagram with some estimates of the lift-drag increments for a full span

N.A.C.A. double slotted flap, roughly comparable with the arrangement on this aircraft, suggests that the same lift increment might have been obtained with about half the observed profile drag increment if a full-span double slotted flap had been used. The full span double-slotted flap was, of course, ruled out by the requirement of providing lateral control by normal ailerons.

The profile drag increment at the half-flap setting appears to be about three times greater than that which could have been obtained with a full span double slotted flap with optimum gap sizes. On this aircraft, no attempt was made to produce the optimum gap size at any but the full flap setting.

Finally, the variation of overall lift/drag ratio with lift coefficient is given in Fig.16, showing that a maximum lift/drag ratio of 7.3 is obtained with flaps up, falling to 5.8 when the flaps are fully extended. The variation of gliding angle with equivalent airspeed is shown in Fig.17, and in Fig.18, the attitude of the aircraft datum to the horizontal is plotted against lift coefficient, for each of the three flap positions. At a gliding speed of 80 knots, with engine off, full deflection of the flaps produces a nose-down change in attitude of nearly 17 degrees, while the gliding angle is increased by just under 2 degrees.

5.4 Trim changes due to flaps and engine power

The results of the measurement of elevator angle to trim at various speeds, flap positions and engine powers are given in Fig.19. It can be seen that in all conditions tested, the stick fixed static longitudinal stability remained positive, the C.G. being at 37% S.M.C.

The changes in elevator angle to trim with different flap positions remain small, both with engine off and with engine on, as shown in the following table. The elevator angles are quoted at a constant airspeed of 80 knots, and also at a constant ratio (1.15) of airspeed to stalling speed (engine off).

Table V

Flap Position	Elevator Angle to Trim			
	Engine Off		Engine On	
	At 80 knots	At 1.15 times Stalling Speed	At 80 knots	At 1.15 times Stalling Speed
Flaps up	2.0° up	2.2° up	0.8° down	0.7° down
Half Flap	2.6° down	1.2° down	-	-
Flaps Down	0.1° down	1.8° up	0.6° down	Neutral

Lowering the flaps produces a small nose-up change in trim with power off, and a very small nose-down change with power on. The effect of the application of engine power is to produce a small nose-up change in trim.

There is a marked reduction in elevator effectiveness at high lift coefficients, at each of the three flap positions, with power off. This deterioration is not apparent with power on, and is presumably associated with the early growth of the stalled region at the wing-fuselage junction. It has already been suggested (in section 5.1) that the flow conditions in this region are improved in the presence of slipstream.

With the above C.G. position, 10° of elevator are required to produce the stall with flaps up, and 5° with the flaps half down or fully down.

Since it was not possible to produce trim curves for more than one C.G. position, only rough estimates of static margin can be made. The elevator effectiveness has been estimated from the charts of Ref.11. The slopes of the trim curves of Fig.17 have been measured over the limited ranges of lift coefficients indicated in the table below, since the slope changes rapidly at higher lift coefficients, particularly with power off.

Then, if a_2 = increment of tailplane lift coefficient per unit elevator deflection

\bar{V} = tailplane volume coefficient

η = elevator angle to trim

C_L, C_M = lift and pitching moment coefficients,

we may write

$$a_2 \bar{V} \frac{d\eta}{dC_L} = \frac{dC_M}{dC_L}$$

where dC_M/dC_L gives the static margin in terms of the standard mean chord, as shown in the following table.

Table VI

$$a_2 = 0.0293 C_L/\text{degree}; \bar{V} = 0.70$$

Flap Position	Engine Condition	C_L range	$d\eta/dC_L$ degrees/ C_L	dC_M/dC_L
Flaps Up	off	0.4 -1.0	-10.0	-0.20
Half Flap	"	0.6 -1.3	-4.6	-0.09
Flaps Down	"	0.9 -2.3	-1.9	-0.04
Flaps Up	on	0.3 -1.0	-4.9	-0.10
Flaps Down	"	0.9 -2.0	-0.6	-0.01

The static margin with flaps up, engine off is seen to be very large, while that with flaps down, and power on is marginal. Lowering the flaps, with power off, moves the neutral point forward an estimated 16% of the mean chord, although the stability remains positive. With power on, the forward shift is 9%. The effect of power

is seen to be destabilising, reducing the static margin by 10% of the standard mean chord with the flaps up, and by 3% with flaps down.

The curves of elevator angle to trim at the same C.G. position (0.376), obtained from the model tests (Ref.2) are also given in Fig.19. It is seen that the actual aircraft is more stable than would be indicated by the tunnel tests, these latter having produced values of dC_M/dC_L of -0.05 with flaps up, and zero with flaps down.

With the C.G. situated at a height of 10% of the mean chord above the standard mean chord line, we should have expected a reduction in stability at high lift coefficients. Over the range of lift coefficients quoted in the above table, the effect of reducing the C.G. height to zero would be to increase the static margins by about 2% of the mean chord in all cases.

All the above estimates of dC_M/dC_L are intended to give only a rough indication of the movement of the neutral point with variation in flap angle and power setting. An over-estimate of elevator effectiveness may account for the apparently very large static margin with flaps up, power off.

5.5 Ground Effect on Pitching Moments

The results of the landing tests which were made to provide information on the effect of ground on pitching moments are given in the table below. The effect of the ground has been expressed as the difference between the elevator angle actually used to achieve the usual 3-point attitude at touch down, and the elevator angle to trim at the same incidence in free flight, away from the influence of the ground. It has been assumed that the aircraft was in trimmed level flight just before touch-down.

Table VII

Flap Position	Approach ($\frac{1}{3}$ Power on)			Touch-down(Power Off)			Elevator Angles		
	I.A.S knots	V/V_{so} *	Elevator Angle (trimmed)	I.A.S knots	Wing Incidence α , degrees	Measured Elevator Angle	Free Flight Elev. Angle, same α	Change due to ground	Overall measured change
Flaps Up	74	1.16	-1.1°	58	10.7°	-7.7°	-1.9°	5.8°up	6.6°up
Half Flap	64	1.16	+1.8°	48	11.0°	-6.3°	-0.3°	6.0°up	8.1°up
Full Flap	63	1.38	-0.1°	35	8.7°	-12.0°	-1.7°	10.3°up	11.9°up

* Note:- V = equivalent airspeed in approach, knots

V_{so} = stalling speed, engine off, knots.

With the above assumption regarding the condition of the aircraft at touch-down, it appears that the effect of the ground, at an incidence of about 10 degrees, is to produce a nose-down pitching moment requiring an extra 6 degrees of up-elevator with flaps up or half down, and an extra 10 degrees with flaps fully down. It also

appears that this ground effect accounts for the major part of the elevator movement required to achieve the touch-down attitude.

If, instead of being in level flight just before touch-down, the aircraft is assumed to be descending with an angle of glide of, say, 2 degrees, then the incidence will have been underestimated by this amount. The nett effect would be to reduce the estimate of the effect of ground to 4 degrees of elevator in the flaps up or half down case, and making no appreciable difference to the flaps down case.

The only conclusion drawn from this rough investigation is that the effect of ground is not large, and that there is ample elevator power to make a 3-point landing, with flaps down.

5.6 Lateral Control Characteristics

5.6.1 Rates of Rotation

Rates of roll and yaw, converted to rates about wind axes, were obtained at a range of speeds and aileron deflections, in each of the three flap positions. It was found that, at a given speed, the steady rate of rotation was proportional to the aileron deflection from the trimmed position, and the rates given in Fig.20 correspond in all cases to an aileron deflection of 15 degrees.

In this diagram, the rates of roll and yaw are expressed in the dimensionless forms $pb/2V$ and $rb/2V$ respectively, where p and r are rates of roll and yaw (radians per second), b is the wing span (feet) and V is the true airspeed (feet per second). Each of the plotted points was obtained from several measurements at each speed, from which the rate of roll or yaw corresponding to the standard 15 degree control deflection could be obtained graphically.

Fig.21 is a typical time history of one such roll manoeuvre. The rates of roll and yaw used in the preparation of Fig.20 were in all cases measured at the points where the rates first became steady, although, in the case of the rate of roll, this was not necessarily the maximum value recorded. Slight spiral instability is indicated by the continued increase in rate of roll after the initial steady value had been reached. This time history is discussed in more detail in Section 5.6.2.

Returning to Fig.20, it is seen that a $\frac{pb}{2V}$ of almost 0.1 is maintained up to the highest lift coefficients at which measurements were made, and there is a tendency for $\frac{pb}{2V}$ to increase in this region.

This may have been due to wing-tip stalling, induced by the higher effective incidence of the down-going wing tip, and so reducing the damping. Since the ratio $pb/2V$ is equal to the tangent of the increase in incidence of the down-going wing tip, this increase amounts to over $5\frac{1}{2}$ degrees at $pb/2V$ of 0.1. If, therefore, the overall wing incidence is within 5 or 6 degrees of the stall, there appears to be a possibility that the wing tip may stall when the rate of roll has developed. The lift coefficients at which this might occur are about 1.0 with flaps up and 2.0 with flaps down. The corresponding increases in $\frac{pb}{2V}$ are observed to occur at lift coefficients of 0.9 and 1.7 with flaps up and down respectively.

The decrease of $pb/2V$ at the high speed end of the flaps-up curve is indicative of the existence of a finite aileron reversal speed. This curve has been extrapolated to zero $pb/2V$ at the lift coefficient corresponding to the estimated reversal speed. The method of estimation is given in Section 5.6.3.

If $pb/2V$ is plotted against the ratio of airspeed to the stalling speed appropriate to the flap position, the three curves are almost coincident, as can be seen in Fig.22. At airspeeds below 1.15 times the stalling speed, $pb/2V$ is increasing fairly rapidly and there may be a danger of autorotation if large aileron deflections are used at lower speeds. This danger, however, is unlikely to arise during a low speed approach to land, since an appreciable time is required for the maximum rate of roll to develop.

The aileron power, expressed as the rate of roll per unit aileron deflection, is shown in Fig.23 as a function of airspeed. The upper diagram covers the low speed end of the range, while the lower diagram covers the whole speed range for which measurements were made with flaps up. The aileron power was just starting to decrease at the highest flight test airspeed (180 knots) and the maximum occurred at about 175 knots.

The maximum rates of adverse yaw, expressed as $rb/2V$, are shown in Fig.20, as functions of the lift coefficient for each flap position. These rates show a general increase with increase in lift coefficient, maximum values of $rb/2V$ of 0.03 being obtained in each case. This amount of adverse yaw was considered by some pilots to be objectionable, particularly when attempting to hold the wings level as the stall was approached.

It is of interest to consider how this yawing behaviour affected the attainable rate of roll, in order to determine what rolling performance would have been attainable if the yawing had been controlled with the rudder.

It has been assumed that the correction to the rolling helix angle, $\Delta(pb/2V)$ is given approximately by the equation

$$\Delta(pb/2V) = -\beta \ell_v/\ell_p + (rb/2V) \ell_r/\ell_p.$$

where β is the angle of sideslip and ℓ_v , ℓ_p and ℓ_r are respectively the rolling moment derivatives due to sideslip velocity, rate of roll and rate of yaw. The validity of this assumption has been checked by some calculations of the response of an aircraft in both roll and yaw to various applied rolling and yawing moments.

It is concluded that if this correction is applied to the measured instantaneous rate of roll, the resulting time history corresponds reasonably closely to the curve that would be expected under pure rolling conditions, at least for the first 1-2 seconds of the motion. On the Youngman-Baynes aircraft, for which ℓ_v is very small, the correction amounts roughly to the addition of between 0.5 and 1.5 times $(rb/2V)$ to the measured value of $(pb/2V)$, depending upon the value of ℓ_r (which is roughly proportional to C_L). The derivatives were estimated from the charts of Ref.12. The gross rate of roll is thus roughly equal to the sum of the measured rates of roll and adverse yaw,

and is adequate in all conditions of flight, particularly if rudder is used to control the adverse yawing. For example, at the mean lift coefficient used on the approach to land, with flaps down, the use of rudder in this way would increase the available $pb/2V$ (Fig.20) from 0.093 to 0.108.

5.6.2 Response

This section is concerned with the lag and sluggishness of the ailerons, so that it is first necessary to define these two terms. The definitions adopted by Young in Ref.13 are as follows. The lag is defined as the time that elapses after a control is moved before the aircraft begins to respond to the movement. The sluggishness is conveniently, if roughly measured by the time that elapses (less any lag) after the control has been displaced before the rolling moment reaches its full value. This latter definition is not altogether satisfactory for this aircraft, since the rate of roll had usually reached, say, $\frac{3}{4}$ of the maximum value in about half the time taken to reach the maximum.

Referring to Fig.21, the ailerons start to move at point A on the time scale, and the rate of roll starts to develop at point B. The time interval AB therefore represents the lag. The aileron reaches its maximum deflection at point C, and, allowing for the lag, the sluggishness is measured from point D to point E, where the rate of roll first becomes steady.

With the above definitions, the lag and sluggishness have been measured from the records obtained at a range of speeds and aileron deflections, and mean values are quoted in the following table, together with the corresponding maximum and minimum values.

Table VIII

Flap Position	Lag, Secs.			Sluggishness, Secs.		
	Minimum	Mean	Maximum	Minimum	Mean	Maximum
Up	0.05	0.09	0.16	0.52	0.77	1.09
Half Down	0.06	0.11	0.16	0.51	1.06	1.59
Full Down	0	0.11	0.25	0.81	1.05	1.71

It is suggested in Ref.13, from an analysis of American flight tests, that a lag of 0.1 seconds is unnoticed by the pilots while a lag of 0.25 seconds is objectionable. Similarly, a sluggishness of 0.1 seconds was considered satisfactory, while 0.4 seconds was objectionable.

The lag on the above aircraft is therefore considered to be satisfactory, but it appears that the sluggishness is excessive. No complaints on this point were, however, made by any of the pilots, in spite of the fact that the measured sluggishness is 10 times the recommended value. The reason probably lies in the method of defining sluggishness. The pilots were probably unaware of the instant at which

the rolling velocity reached the maximum value, but may have been more concerned with the time taken for the angle of bank to reach some chosen value. The relation between the angle of bank and the time measured from the start of the control movement is shown in Fig.24. The upper curve refers to an airspeed of 1.15 times the engine-off stalling speed, and the lower one to a constant speed corresponding to a lift coefficient of 1.0. From this it is seen that 20 degrees of bank can be applied in under $1\frac{1}{2}$ seconds during a flaps-down approach to land, or in half that time at about 80 knots, irrespective of the flap position. Since the aileron control, even at low speeds, with flaps down, was never criticised on the grounds of sluggishness, it is suggested that the definition used earlier in this section is less realistic than one based on the time to bank, say, 20° , and that this time should not exceed 1.5 seconds. By comparison, a proposed requirement for deck-landing aircraft (Ref.14) stipulates a time not exceeding 0.75 seconds for the application of 10 degrees of bank, at a speed of 1.15 times the (engine on) stalling speed. In this condition, a Seafire IIC aircraft recorded a time of 0.75 seconds for 10 degrees of bank and 1 second for 20 degrees of bank. The lateral control on this aircraft was considered to be good.

5.6.3 Aileron Reversal Speed

From measurements of aileron power, expressed as the rate of roll per unit aileron deflection, at a range of speeds up to the highest practicable speed, the aileron reversal speed has been predicted, using the method given in Refs.5 and 6.

For a rigid aircraft, aileron power as defined above, is directly proportional to the airspeed, V . For an elastic aircraft, however, since the aileron power must become zero at the aileron reversal speed V_R , it is assumed that, since wing torsion and its effects tend to vary roughly as V^2 , the aileron power is further proportional to the factor $(1 - V^2/V_R^2)$, so that the aileron power p/ξ is given by

$$p/\xi = kV (1 - V^2/V_R^2)$$

where k is a constant for a given aircraft.

This equation may be re-written in the form

$$p/\xi V^3 = k (1/V^2 - 1/V_R^2)$$

so that if we plot $p/\xi V^3$ against $1/V^2$, a linear relation should be obtained, from which $1/V_R^2$ (and thus the aileron reversal speed) can be obtained.

This has been done in Fig.25, each point on this diagram being obtained from the corresponding point on the curve of $pb/2V$ versus C_L as for the flaps-up case in Fig.18. It can be seen that the relation between $p/\xi V^3$ and $1/V^2$ is reasonably linear, at least at the important high speed end, and the extrapolation to zero aileron power yields an aileron reversal speed of 296 knots. This figure may be compared with the estimated reversal speed of 220 knots (Ref.15), based on measured values of the wing and flap torsional stiffness, and an estimated value of the torsional stiffness of the flap root constraint.

By differentiating the above expression for aileron power it is seen that aileron power should be a maximum at a speed equal to

$V_R/\sqrt{3}$, which in this case, is 171 knots. In fact, the measured maximum, in the lower diagram of Fig.21, occurred at 175 knots.

An attempt was made to measure the twist produced in the main flap when the ailerons were deflected at high speeds. The technique employed (desynn transmitters at each end of each main flap) was not sufficiently sensitive, however, to record any appreciable amount of twist, although it is believed that a twist of $\frac{1}{4}$ degree along the length of the flap should easily have been detectable. It is possible that most of the deflection occurred in the flap root anchorage, where it would not be recorded.

5.7 General Handling Qualities

Although this was purely a research aircraft, and, as such, might not be expected to possess the standard of handling qualities usually required on normal aircraft of this size and weight, it was, nevertheless, very well liked by most of the pilots who flew it.

The take-off, usually made with flaps up, was easy and straightforward. No measurements of take-off distances were made, due to lack of time, but the distance was not considered to be excessive.

The climb performance was generally criticised, and a more powerful engine would have been appreciated. The measured rate of climb at 5000 feet, and the estimated rate at sea level, are given in Fig.26 with flaps up and flaps fully down at an A.U.W. of 3,700 lb. The service ceiling was about 8000 feet (compared with 14,000 feet for the standard Proctor). Above about 1000 feet, it was impossible to maintain height with flaps fully down, and a baulked landing in this condition was impossible.

The normal flying qualities of the aircraft were quite satisfactory. The controls were generally light and effective, though the ailerons tended to become heavy at high speeds. The elevator and rudder trimmers were adequate, but since no aileron trimmer was provided, the aircraft could not be flown "hands-off".

The aileron control in particular was effective right down to the stall, at all flap positions, and the wings could be held level until the actual stall occurred. The adverse aileron yaw was, however, becoming slightly unpleasant in this condition.

The recovery from the stall sometimes took rather a lot of height, and on one occasion over 1000 feet was lost before level flight was resumed. A considerable pull force was required to recover from the steep dive following the stall, with flaps down.

Landing the aircraft was considered to be easy. Landings were usually made with flaps either half down or fully down, although the attitude on the approach with flaps fully down was rather unusual. The view ahead was, however, excellent. Full use was not usually made of the available maximum lift coefficient for landing. The average approach speed with flaps fully down was about 1.4 times the stalling speed, but, with flaps up, or half down, a ratio of 1.16 was normal. At these speeds, a 3-point touch-down could be made, with little or no float. The speed loss during the check with flaps down was large, the A.S.I. reading at touch-down being about equal to the indicated stalling speed. This probably accounts for the use of such a relatively high

speed on the approach, with the flaps fully down. These landings were, however, made with only a small amount of engine on. If flat, engine-on approaches were used, much less speed would have been lost in the check, and a lower approach speed could have been used.

6 Conclusions

(1) Flight tests on the Youngman-Baynes Experimental high lift aircraft have shown that an increment of maximum lift coefficient of 1.32 can be obtained on an unswept low drag section wing with a flap arrangement which, when retracted, barely disturbs the normal wing profile. While the total maximum lift coefficient of 2.60 is not phenomenal, it has been obtained, without increase in stalling incidence, on an aircraft whose maximum lift coefficient with flaps retracted is only 1.28.

It is suggested that an increment of maximum lift coefficient of 0.2 has been lost due to the adverse effect of wing-fuselage interference, and it is thought that this loss would not occur with a moderately tapered wing mounted in the mid- or high-wing position on the fuselage.

(2) The lateral control provided by the ailerons inset in the full span flap gave adequate rolling power and satisfactory response down to the stall, at all flap positions.

(3) The profile drag coefficient increments of the flap were measured to be 0.023 for a lift coefficient increment of 0.45 (at half flap) and 0.071 for a lift coefficient of 1.14 (at full flap) at a wing incidence of 10 degrees. The corresponding profile drag coefficient increment measured during the tunnel tests on the 3-dimensional model was 0.062 for a lift coefficient increment of 1.34.

(4) The changes in longitudinal trim due to the flaps were small and easily controlled, with a tail volume coefficient of 0.7. The flaps appeared to cause a considerable loss in longitudinal stability. The true magnitude of this loss, in terms of static margin, is difficult to assess, since there seems to be a marked loss in elevator effectiveness with flaps up as the stall is approached. This results in an apparently very large static margin with flaps up, which falls to reasonable proportions when the flaps are lowered.

(5) Although the effect of ground on longitudinal trim could not be measured directly, sufficient evidence was obtained to conclude that the trim changes were not large, and no difficulty was experienced when landing with the flaps fully down.

(6) The structure of the wing-flap-aileron arrangement on this experimental aircraft was adequately stiff in torsion, and the aileron reversal speed was estimated to be nearly 300 knots.

REFERENCES

<u>No.</u>	<u>Author</u>	<u>Title, etc.</u>
1	Marshall and Powter	Wind Tunnel Tests on a Double Slotted Flap and Inset Aileron fitted to a Semi-Low Drag Wing Section. A. R. C. 10, 231 October 1946

REFERENCES (Contd.)

<u>No.</u>	<u>Author</u>	<u>Title, etc</u>
2	Ross	Wind Tunnel Tests on a Model of the Youngman-Baynes High Lift Experimental Aircraft. A.R.C.12,741 August, 1949
3	Smelt and Davies	Estimation of the Increase in Lift due to Slipstream. R & M No. 1788 February 1937
4	Hartman and Biermann	The Aerodynamic characteristics of Full Scale Propellers having 2,3 and 4 blades of Clark-Y and R.A.F.6. Airfoil Sections N.A.C.A. Report No. 640 1938.
5	Pugsley and Cox	The Aileron Power of a Monoplane R & M No. 1640 April 1934
6	Morris and Morgan	Aileron Tests on Spitfire K.9944 R & M 2507 April 1941
7	Adamson and Barnes	Body Interference on a High Lift Wing A.R.C.4602 January 1940
8	Adamson	Addendum to Report No. BA.1580 - Body Interference on a High Lift Wing. A.R.C.4603 March 1940.
9	Morgan and Morris	Flight Tests of a Youngman Flap on Fairey PL/34 K7555. R & M 2547 June 1941
10	Young	The Aerodynamic Characteristics of Flaps R & M 2622 February 1947
11	Lyons and Bisgood	An Analysis of the Lift Slope of Aerofoils of Small Aspect Ratio, including Fins, with Design Charts for Aerofoils and Control Surfaces R & M 2308 January 1945
12	-	Royal Aeronautical Society Data Sheets.
13	Young	Lateral Control with High Lift Devices, R & M 2583 May 1941
14	Lean and Stott	An investigation into the suitability of proposed A.D.M. tests for deck-landing aircraft. Part I R & M 2407 June 1947
15	Molyneux and Broadbent	Determination of reversal speed of a wing with a partial span flap and inset aileron. A.R.C.13,308 February 1950.

Table IX

Aerodynamic Data - Youngman Baynes Experimental Aircraft

General		Longitudinal Control	
Mean Weight during tests, lb	3700	Tail Surface area (Gross) S' sq.ft.	46.0
S (Gross Wing area) sq.ft.	180	Elevator Area/S'	0.57
Engine	Gipsy Queen 32	l'/\bar{c} (l' = distance, CG to $\frac{1}{3}$ T.P. chord)	2.84
Rated/H.P. at sea level	250	S'/S	0.256
Power loading, lb/b.h.p.	14.8	Tail Volume Coefficient S' $l'/S\bar{c}$	0.7
Wing loading, lb/sq.ft	20.5	Elevator movement	$\pm 30^\circ$
Span loading, lb/sq.ft	3.4	Type of balance	Horn
C.G. position, h (\bar{c} = S/span)	0.367 \bar{c}	Percentage balance	12
Airscrew diameter, feet	7.5	Svick gearing, degrees/inch	5
Airscrew pitch	Fine 11.5 $^\circ$ Coarse 25 $^\circ$	Total trim tab area, sq.ft	1.05
Gear Ratio	1:1	Trim tab angle, max. up/down	19.5 $^\circ$ / 26 $^\circ$
		Tailplane setting to wing chord	-1 $^\circ$
Wings		Directional Control	
Area (gross) S, sq.ft	180	Fin and Rudder area, S'', sq.ft	16.9
Span, 2s, ft	33	Rudder Area/S''	0.75
Mean Chord, \bar{c} , ft	5.45	l''/s (l'' = distance, CG to centroid of S'')	1.05
Aspect ratio	6.05	Fin and Rudder Volume coefficient, S'' l''/Ss	0.099
Dihedral	3 $^\circ$	Rudder movement	$\pm 19^\circ$
Sweepback of $\frac{1}{4}$ c. line	1.9 $^\circ$	Rudder offset	3 $^\circ$ to port
Chord, ft, root	6.40	Type of balance	Horn
tip	4.61	Percentage balance (horn only)	4.5
Section (basic) root	NACA 65,2-214	Pedal gearing, degrees/inch	5
tip	NACA 65,2-212	Trimming tab area, sq.ft	0.20

Table IX (contd.)

Wing twist, root-tip	0°	Trim tab angles, max, port starboard	14.5° 14.5°
Flaps		Lateral Control	
Type	Double slotted		
Maximum Angle, Main	15°	Type of aileron	Frise
Auxiliary	30° extra	Total Aileron area, sq.ft	22.0
Total flap area*/S	0.50	Aileron area/S	0.122
Total Flap chord/local wing chord	0.50	Aileron chord/local chord	0.25
Auxiliary flap chord/ wing chord.	0.25	Aileron span/2s	0.42
Main flap span/2s.	0.96	Aileron angles, max, up	15°
Auxiliary flap span/2s.	0.54	down	15°
Maximum extended chord/c	1.24	Percentage balance	27
		Stick gearing, degrees/inch	4
		Droop, with flaps down,	15°

* including ailerons, which move with main flaps, and droop 15° at full flap deflection.

FIG. 1.

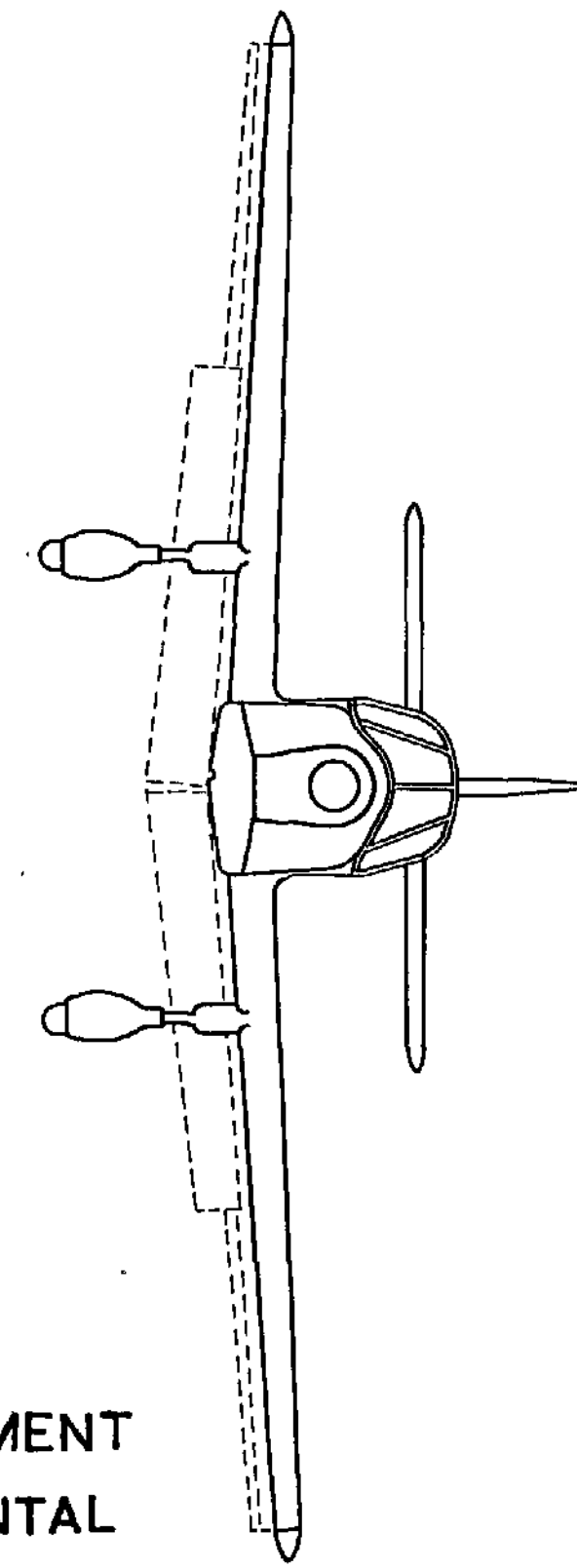
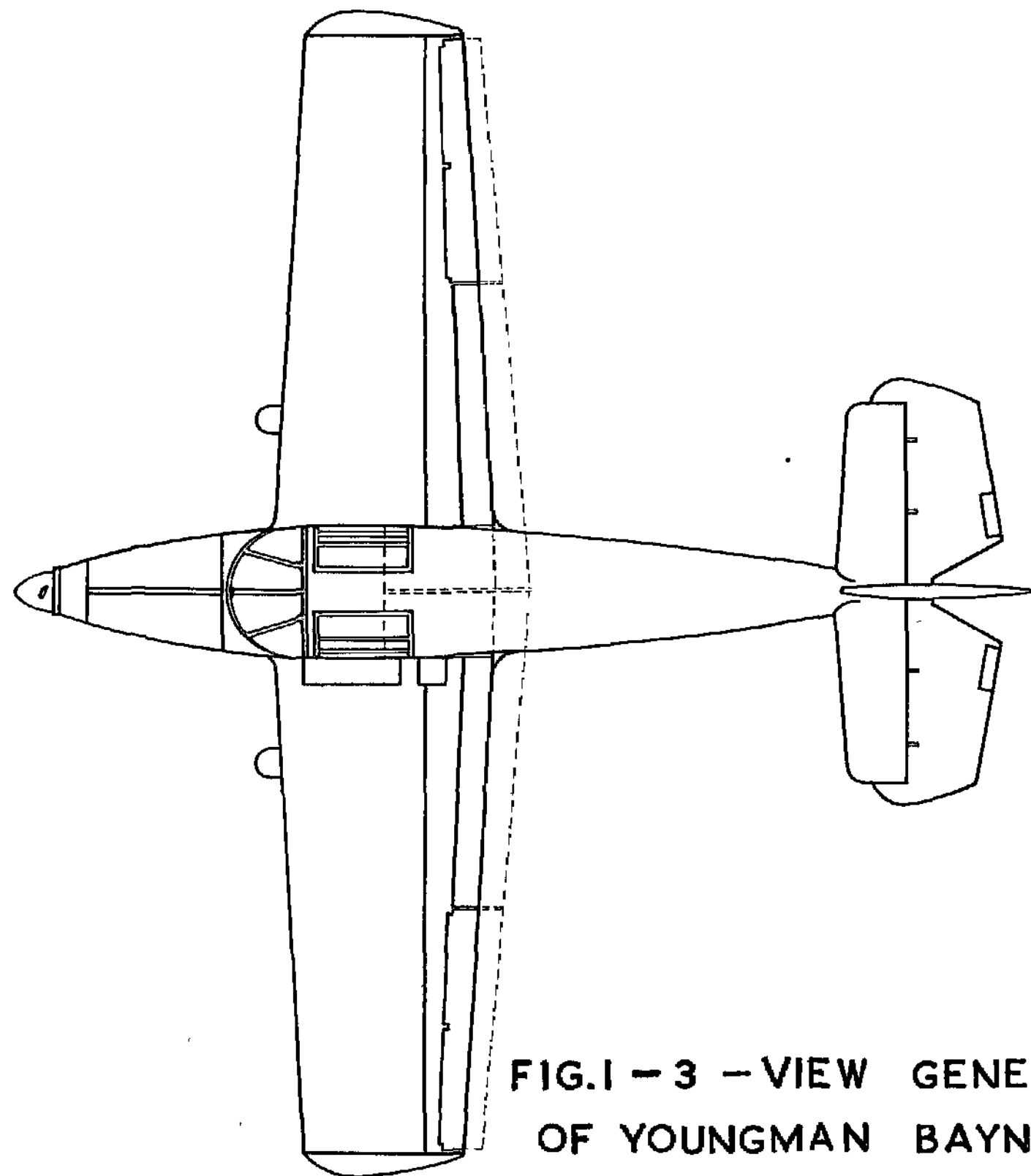
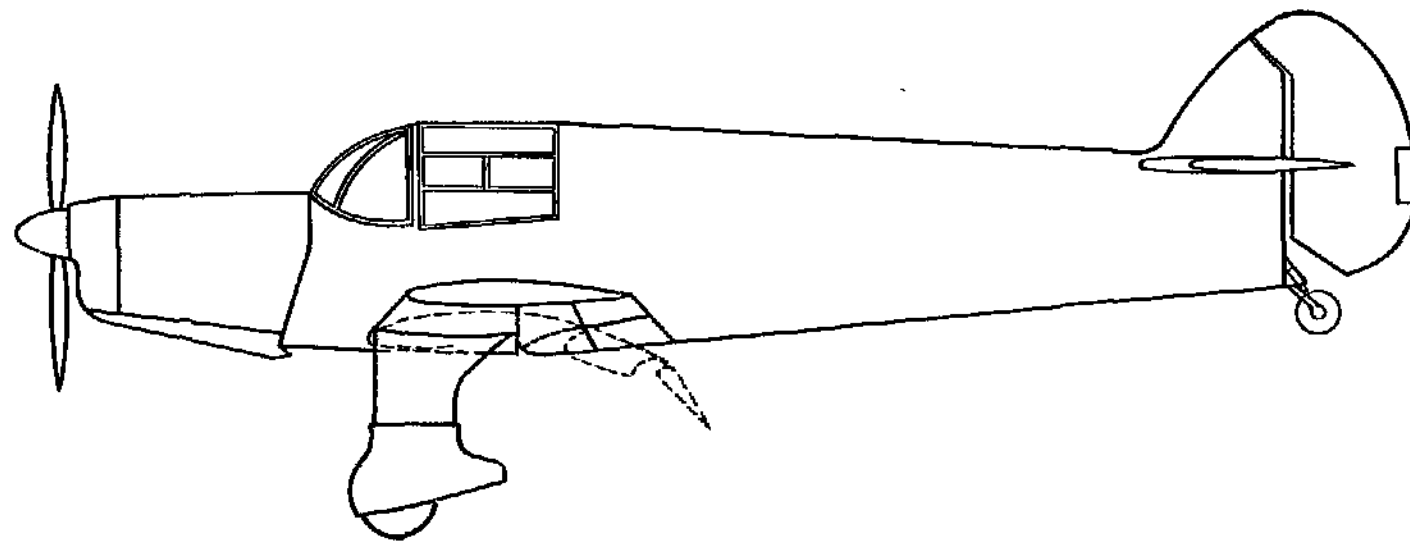
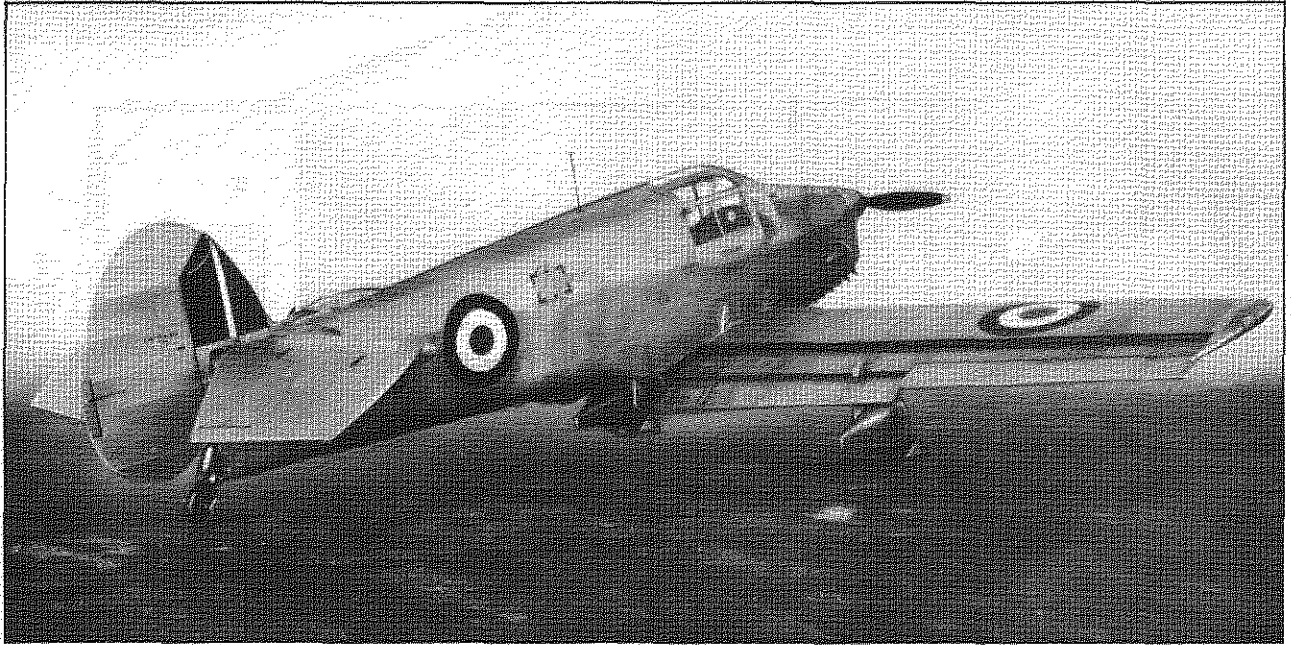


FIG.1 - 3 - VIEW GENERAL ARRANGEMENT
OF YOUNGMAN BAYNES EXPERIMENTAL
HIGH-LIFT AIRCRAFT

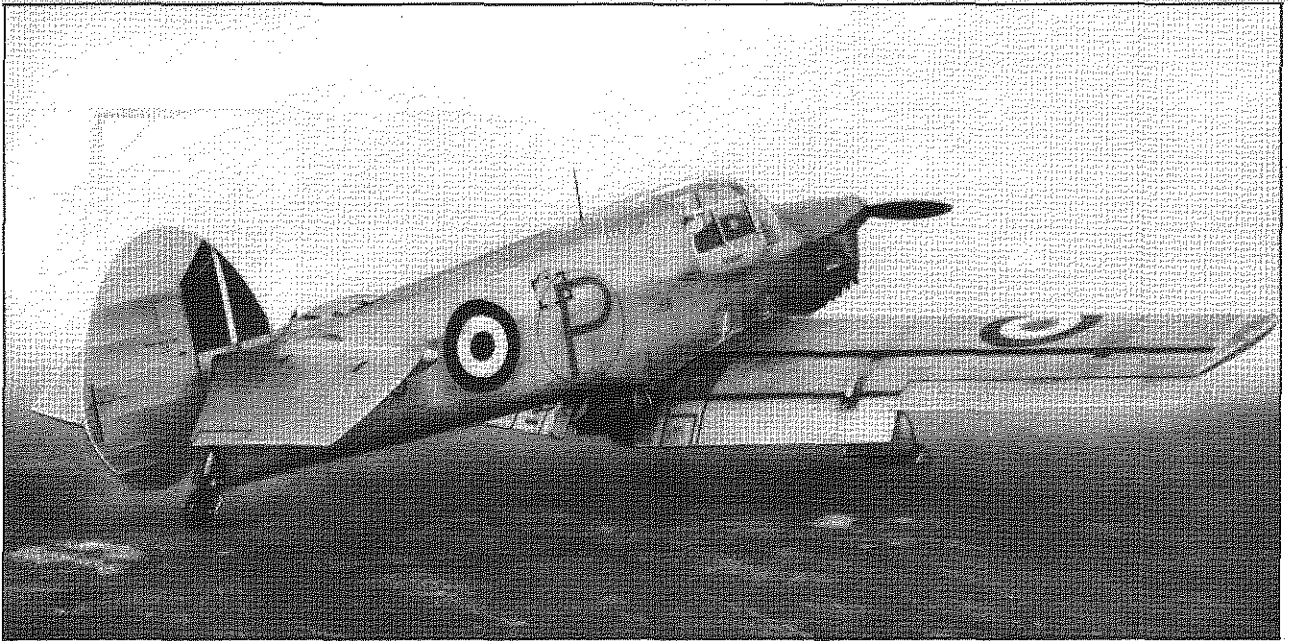
SCALE 1/48



FIG.2. FRONT AND SIDE VIEWS OF YOUNGMAN BAYNES
EXPERIMENTAL AIRCRAFT



A.



B.

FIG.3. REAR VIEWS SHOWING FLAPS EXTENDED

- A. FLAPS HALF DOWN
 - B. FLAPS FULLY DOWN
- } WITH CENTRAL PORTION OF REAR FLAP REMOVED

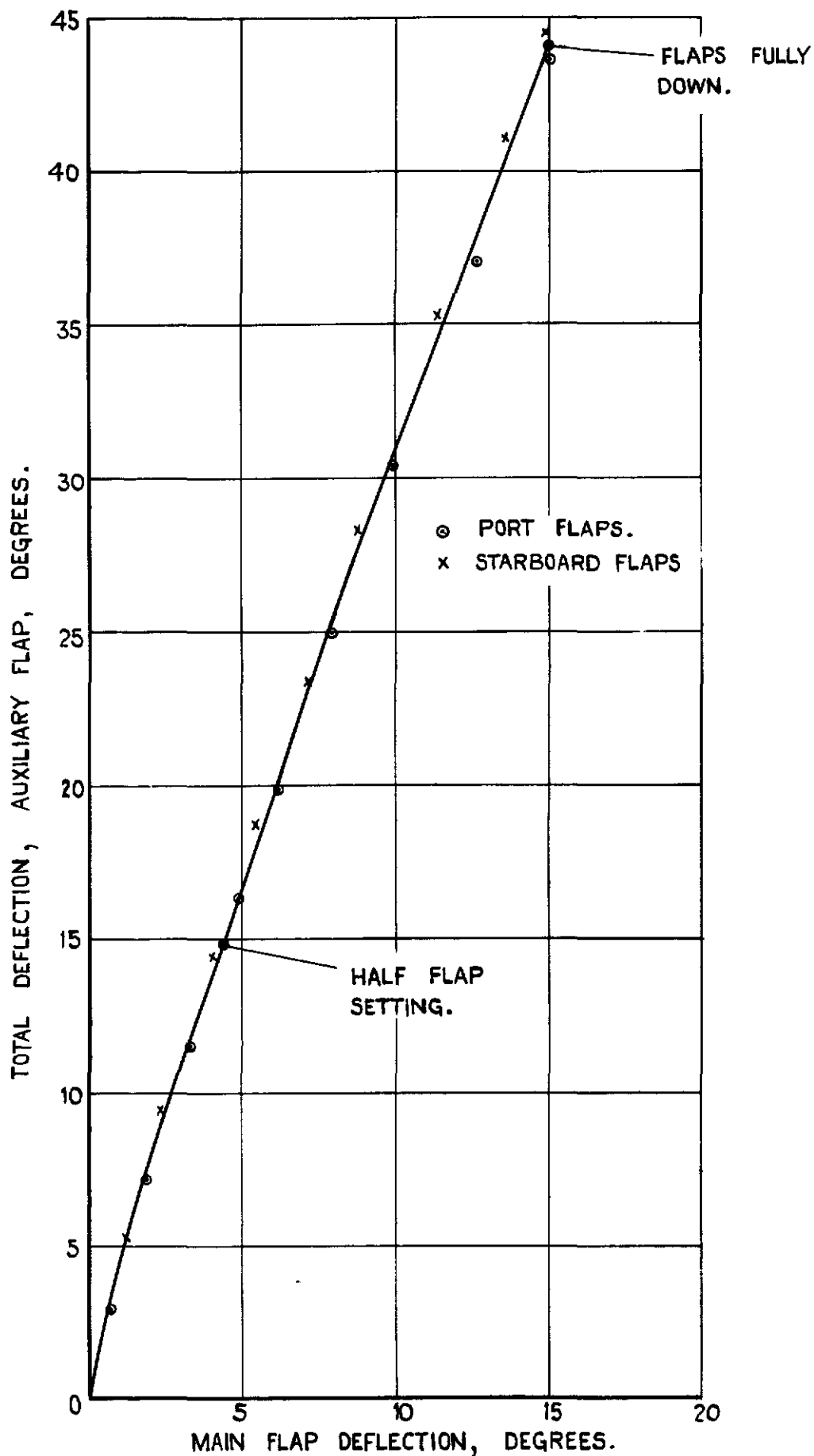


FIG. 4. RELATION BETWEEN MAIN AND AUXILIARY FLAP DEFLECTIONS.

FIG.5.

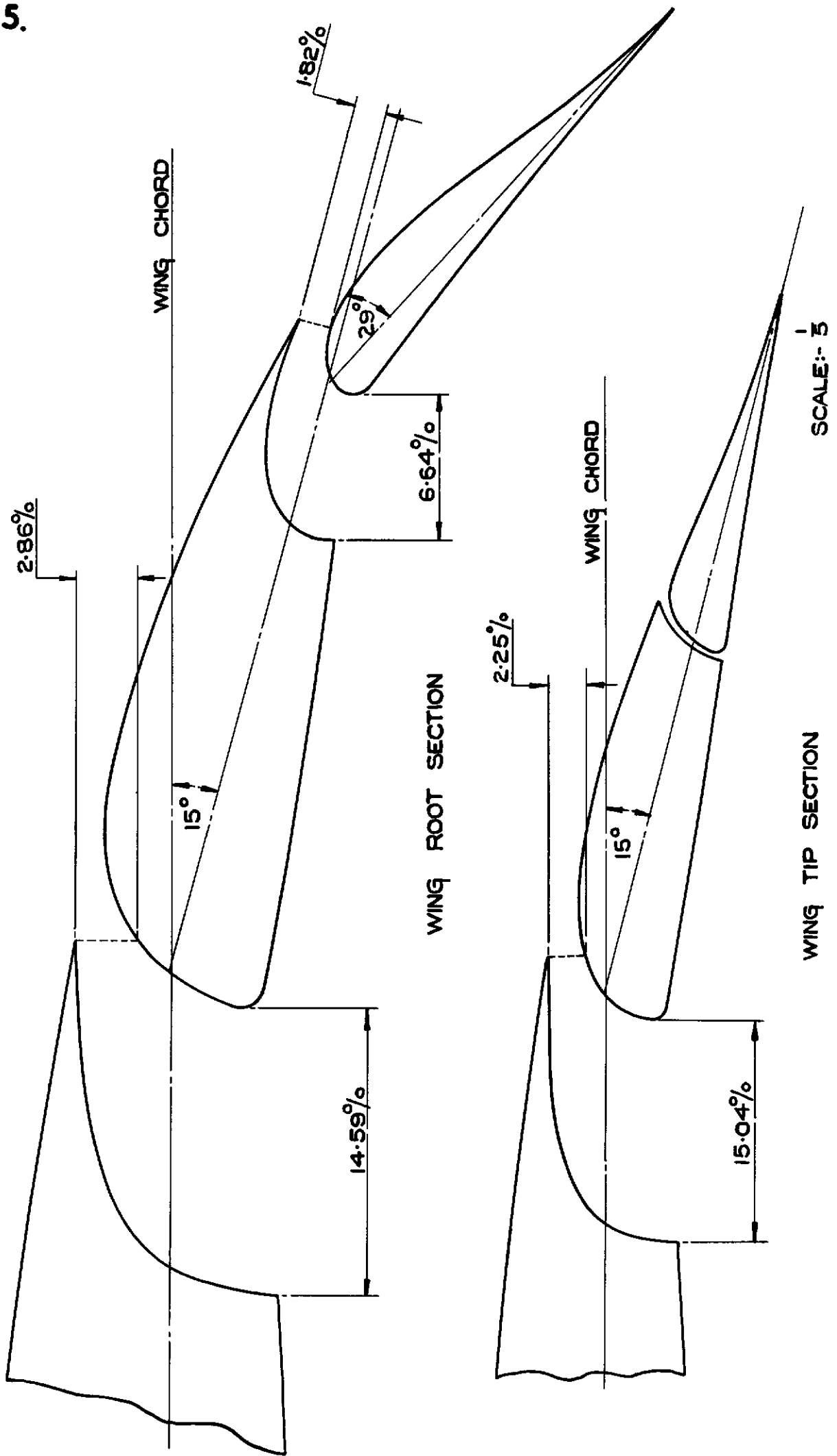
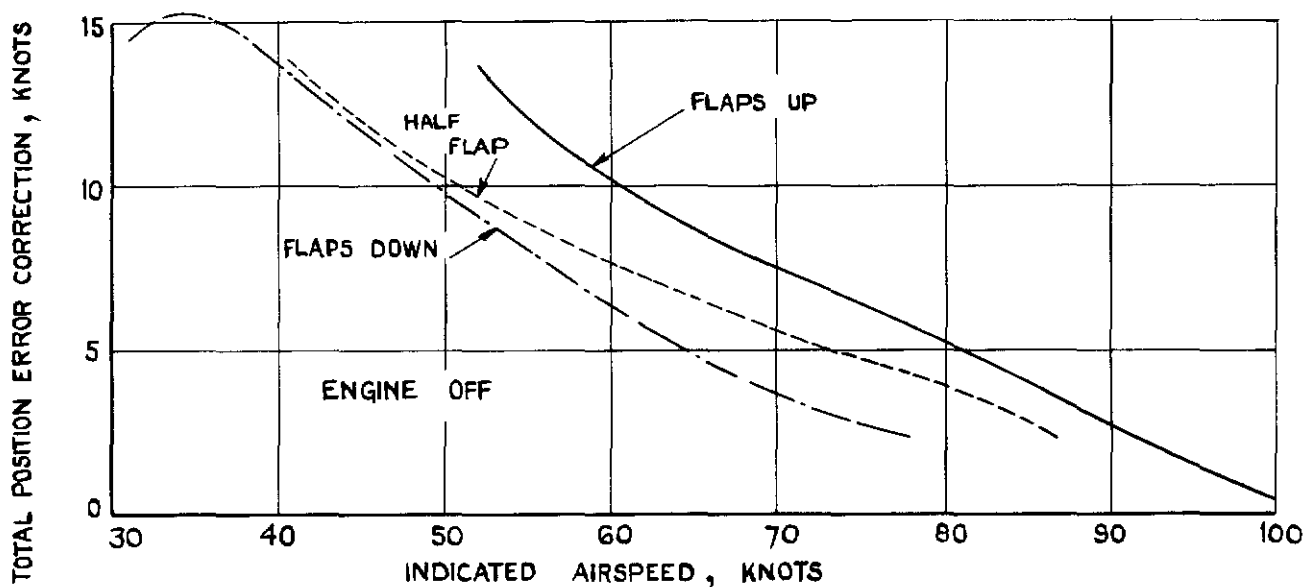


FIG.5. WING SECTIONS AT ROOT AND TIP (FLAPS DOWN) AFTER MODIFICATION.

FIG.6.



A.U.W = 3700 lb

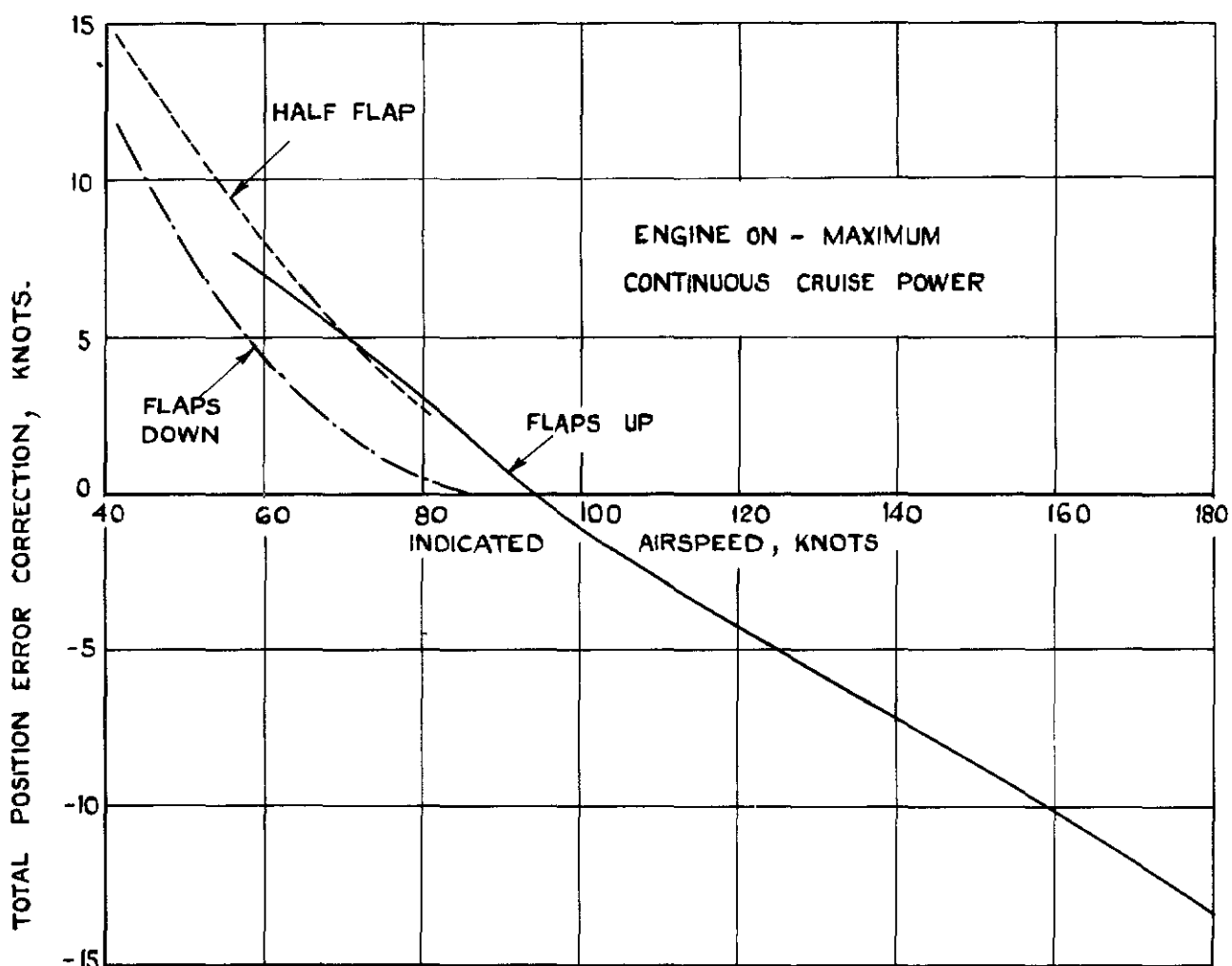


FIG. 6. TOTAL POSITION ERROR CORRECTIONS.

FIG. 7.

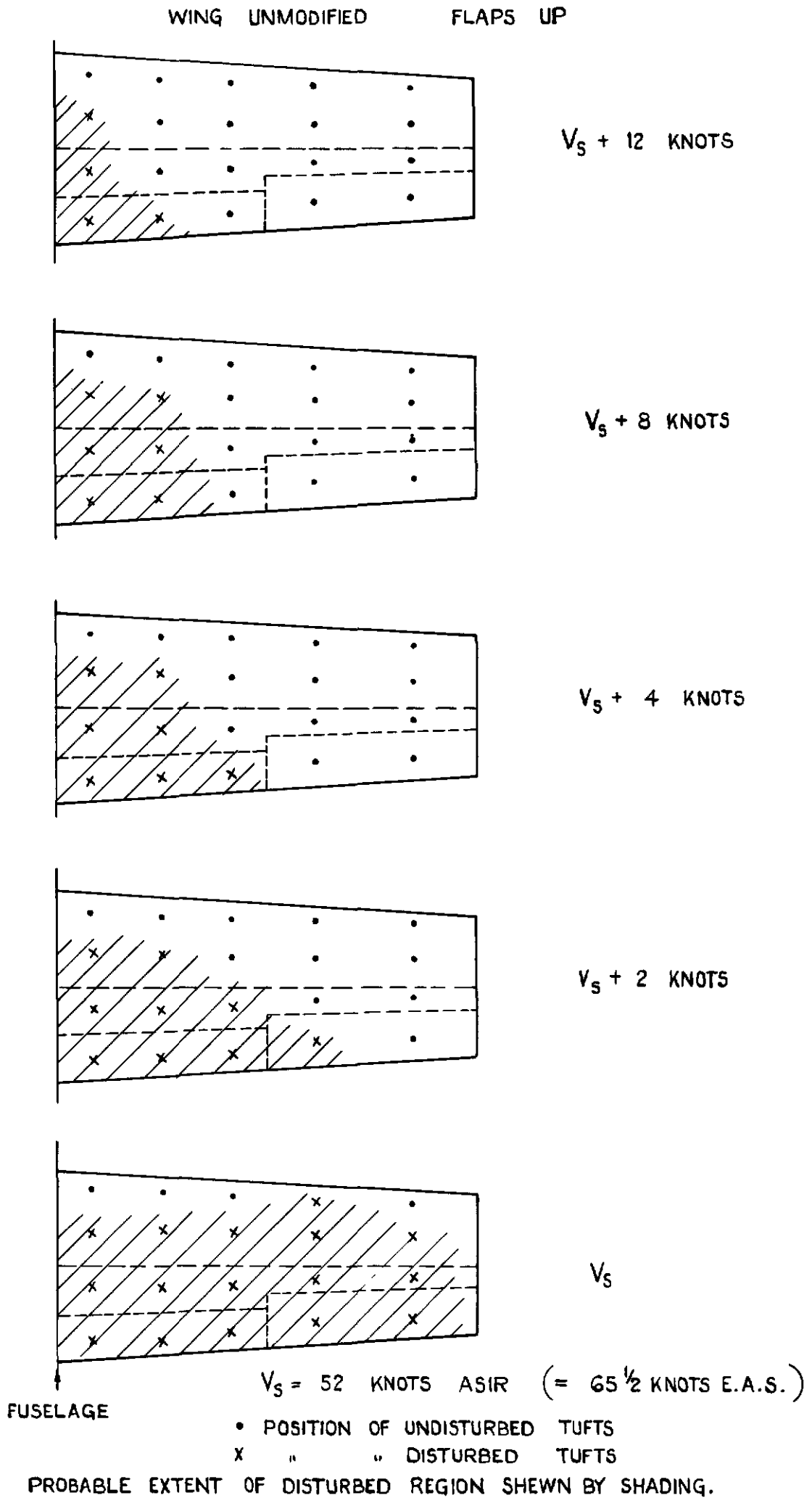
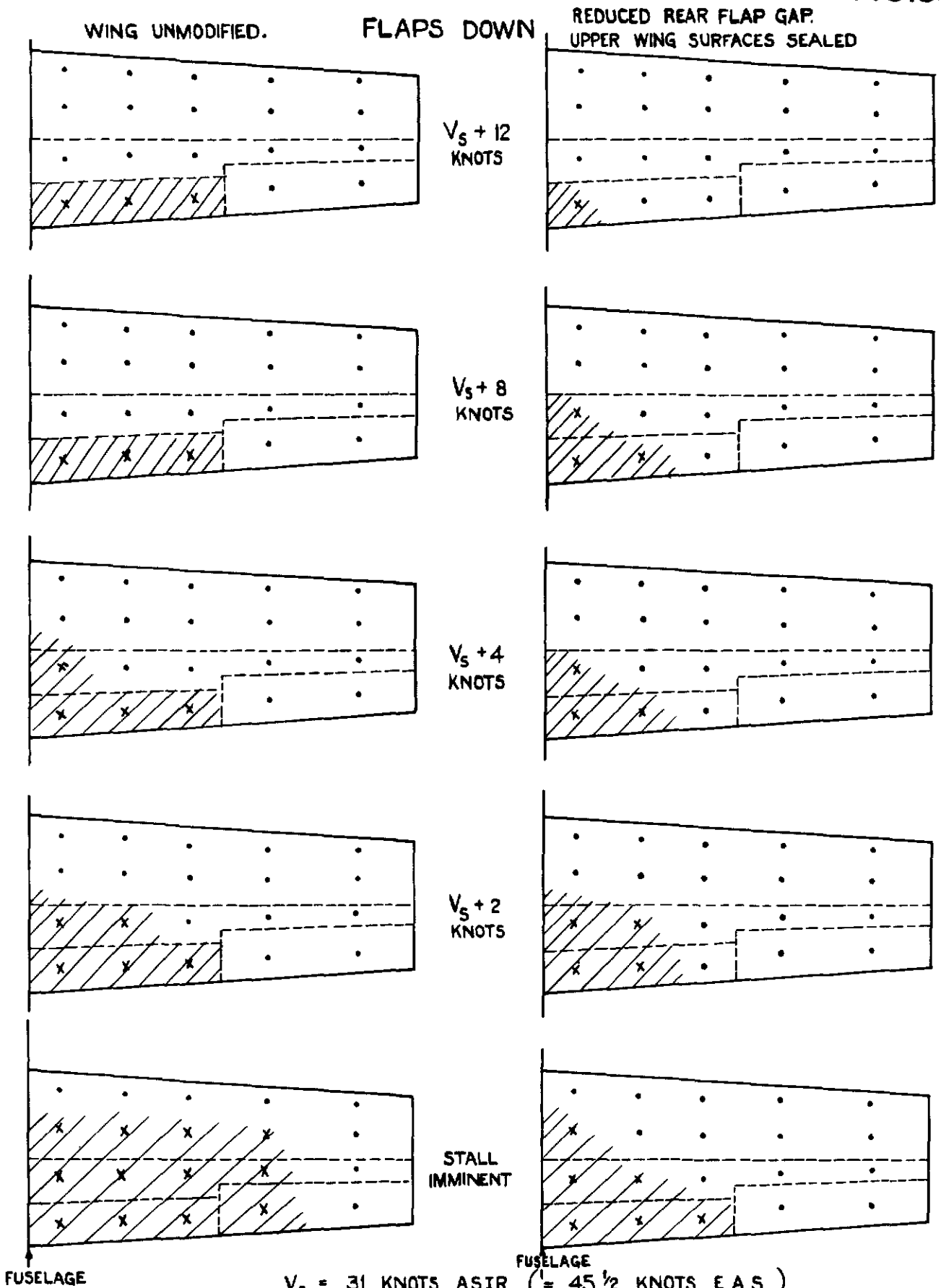


FIG. 7. GROWTH OF STALLED AREA WITH REDUCTION IN SPEED.
 WOOL TUFT OBSERVATIONS — FLAPS UP.

FIG.8.



$V_S = 31$ KNOTS ASIR ($= 45 \frac{1}{2}$ KNOTS EAS)

• POSITION OF UNDISTURBED TUFTS

x " " DISTURBED TUFTS.

PROBABLE EXTENT OF DISTURBED REGION SHEWN BY SHADING

FIG.8. GROWTH OF STALLED AREA WITH REDUCTION IN SPEED.
WOOL TUFT OBSERVATIONS, — FLAPS DOWN.

FIG. 9.

- FLAPS DOWN, ORIGINAL CONDITION
- ◇ HALF FLAP " "
- x FLAPS UP " "
- + FLAPS DOWN, UPPER SURFACE SEALED, REDUCED FLAP GAP

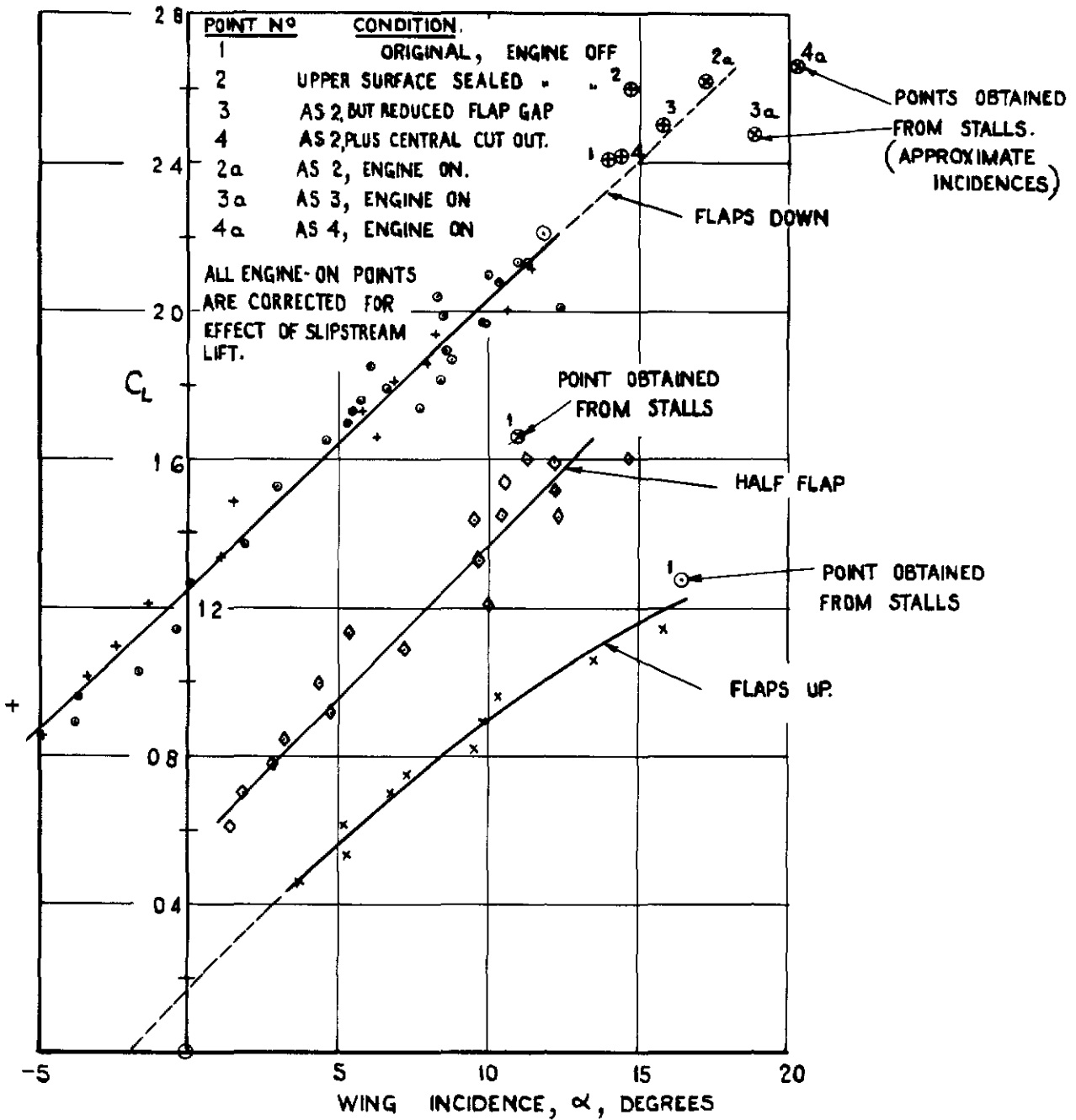


FIG. 9 $C_L - \alpha$ CURVES FROM PARTIAL GLIDE MEASUREMENTS.

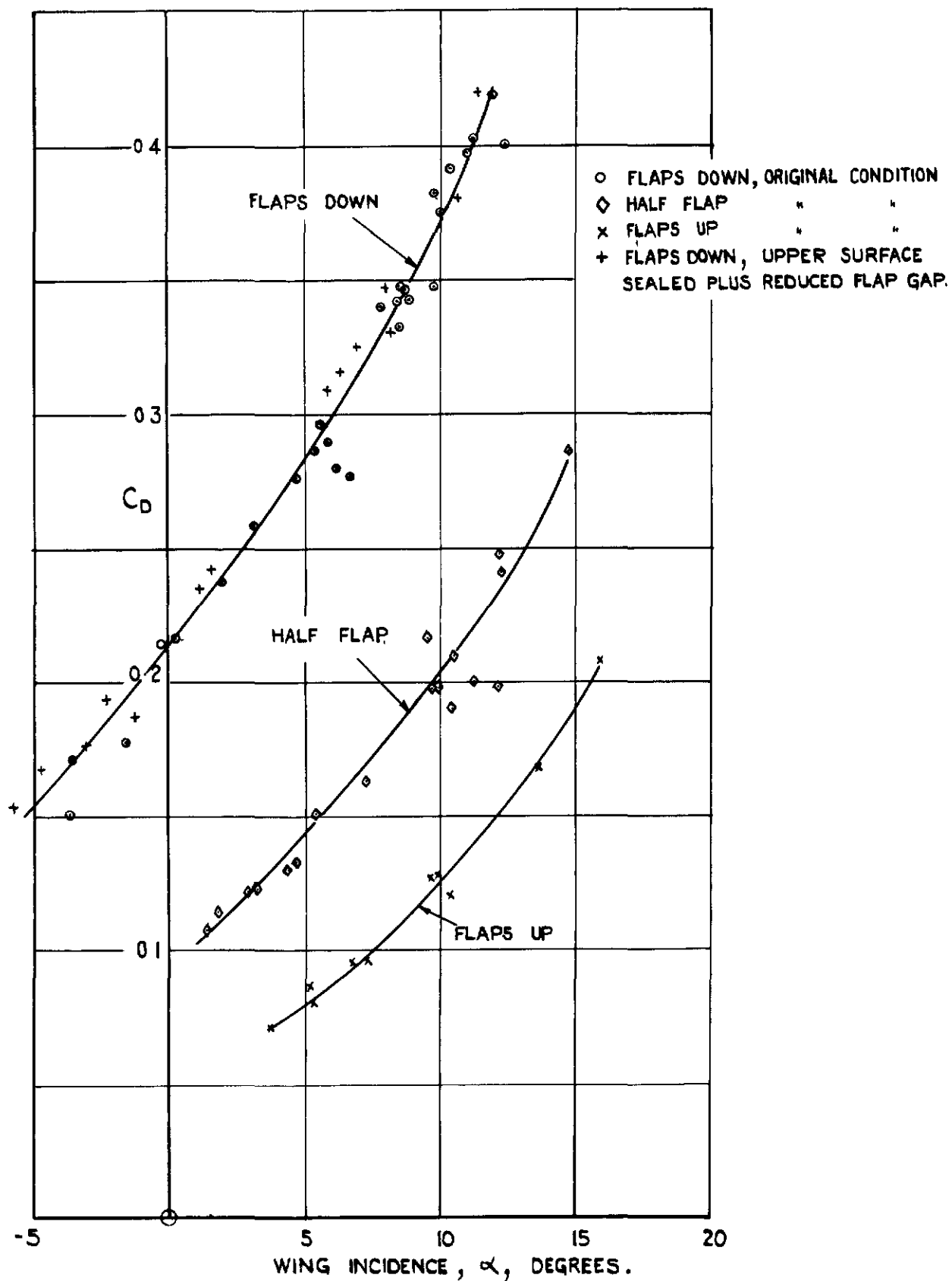


FIG. 10. $C_D - \alpha$ CURVES FROM PARTIAL GLIDE MEASUREMENTS.

FIG. II.

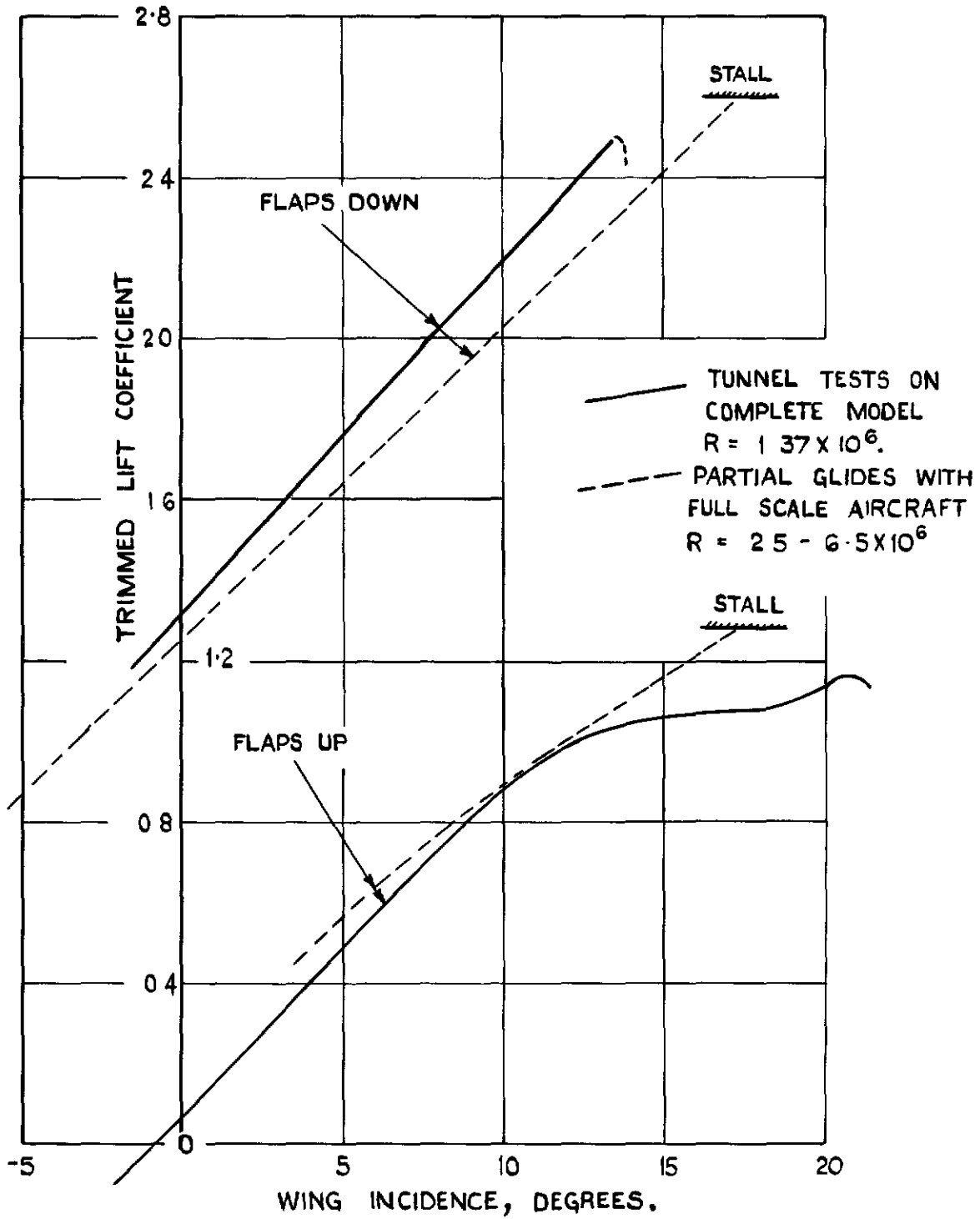


FIG. II. COMPARISON BETWEEN MODEL AND FULL SCALE LIFT CURVES.

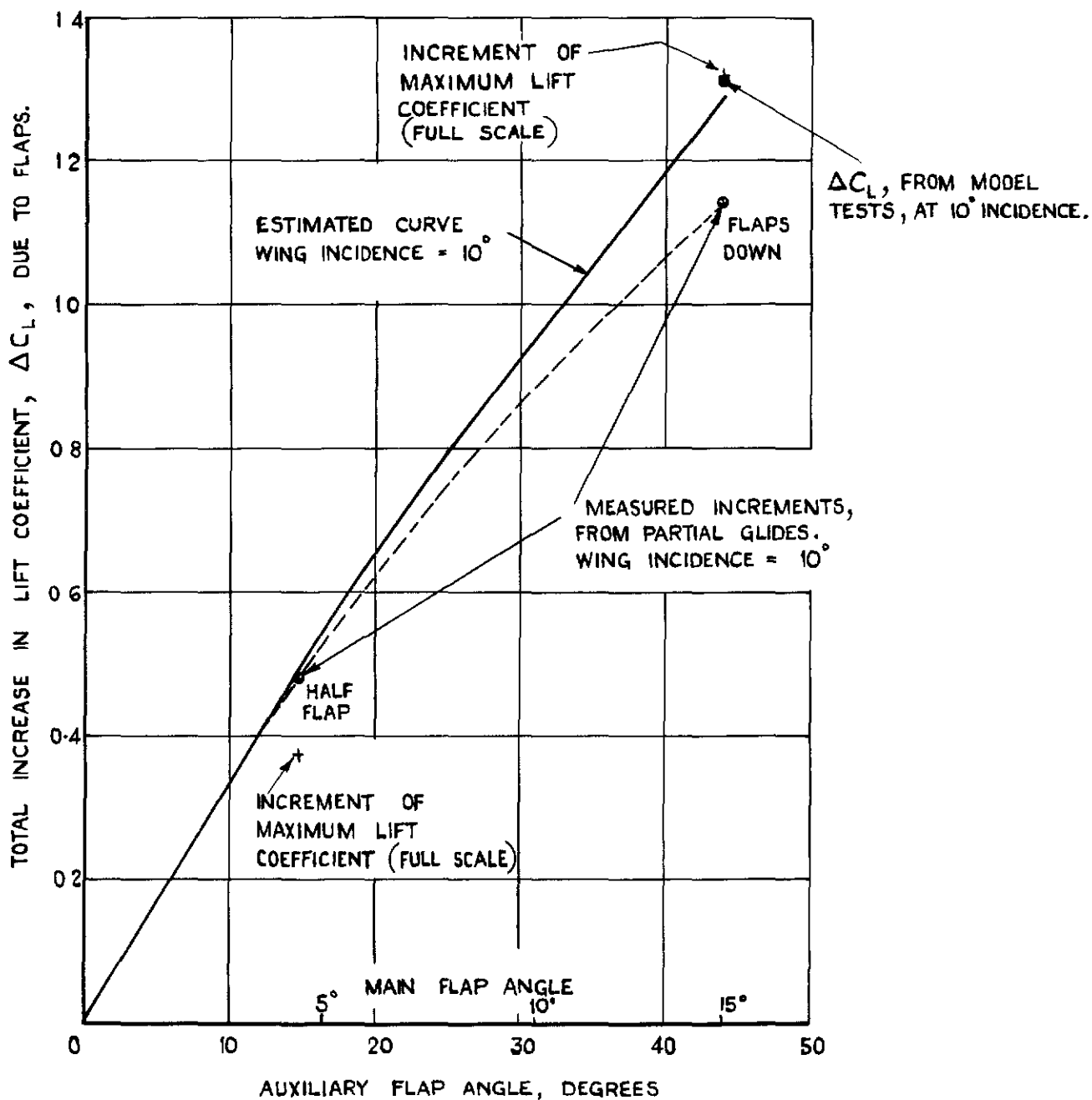


FIG.12 COMPARISON BETWEEN ESTIMATED AND MEASURED LIFT INCREMENTS DUE TO FLAPS.

FIG. 13

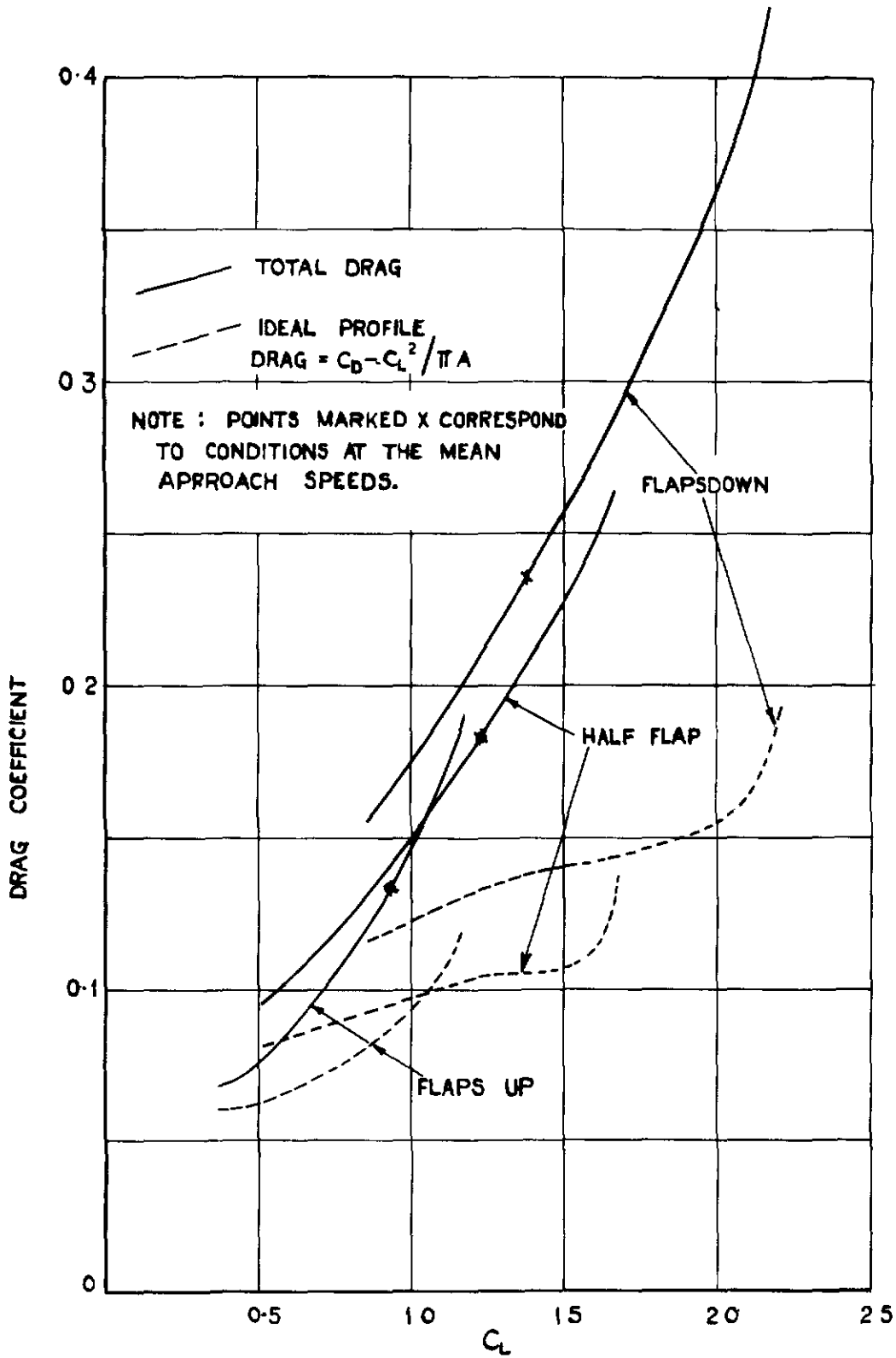


FIG. 13. VARIATION OF TOTAL AND PROFILE DRAG COEFFICIENTS WITH C_L .

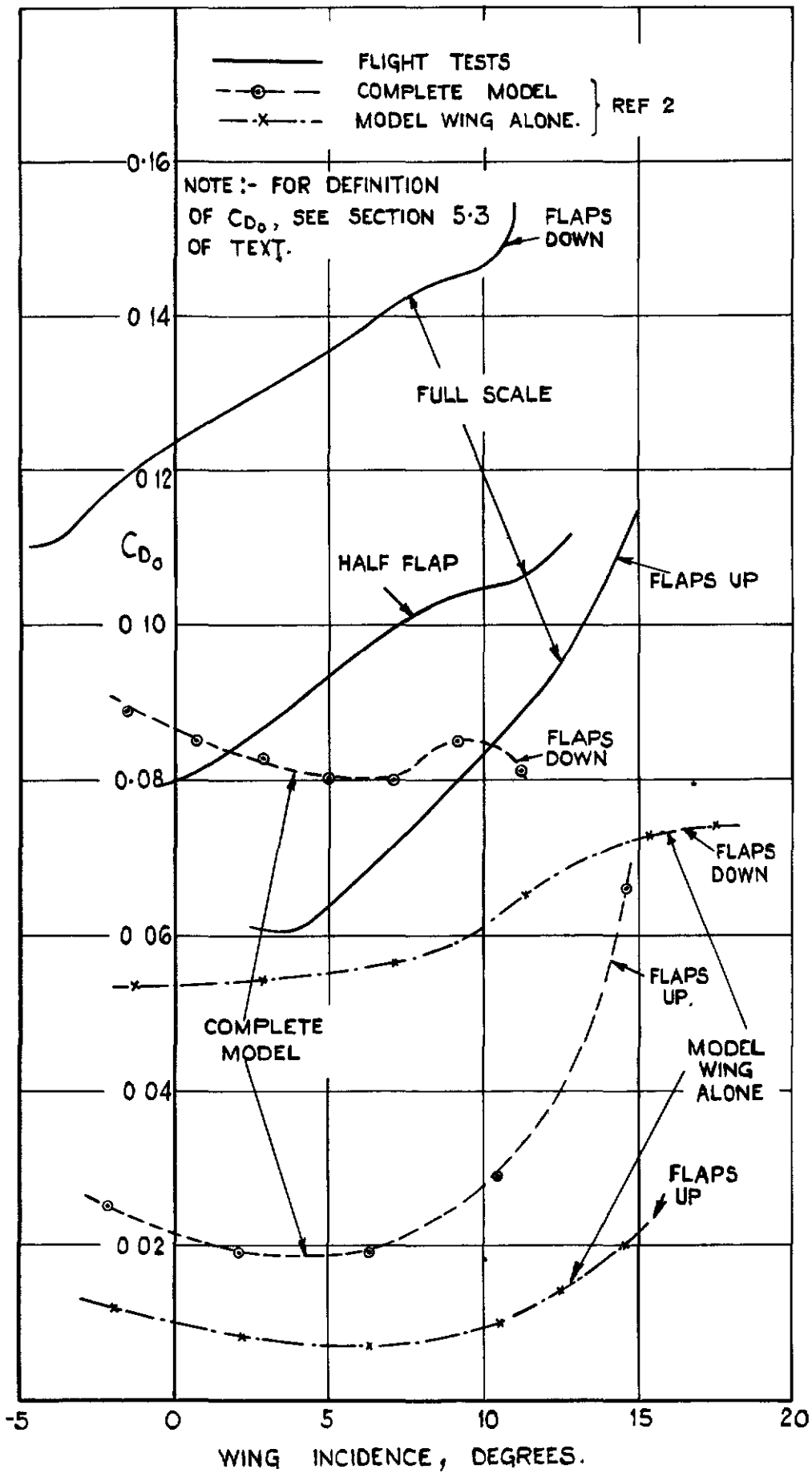


FIG.14. VARIATION OF PROFILE DRAG COEFFICIENT WITH WING INCIDENCE.

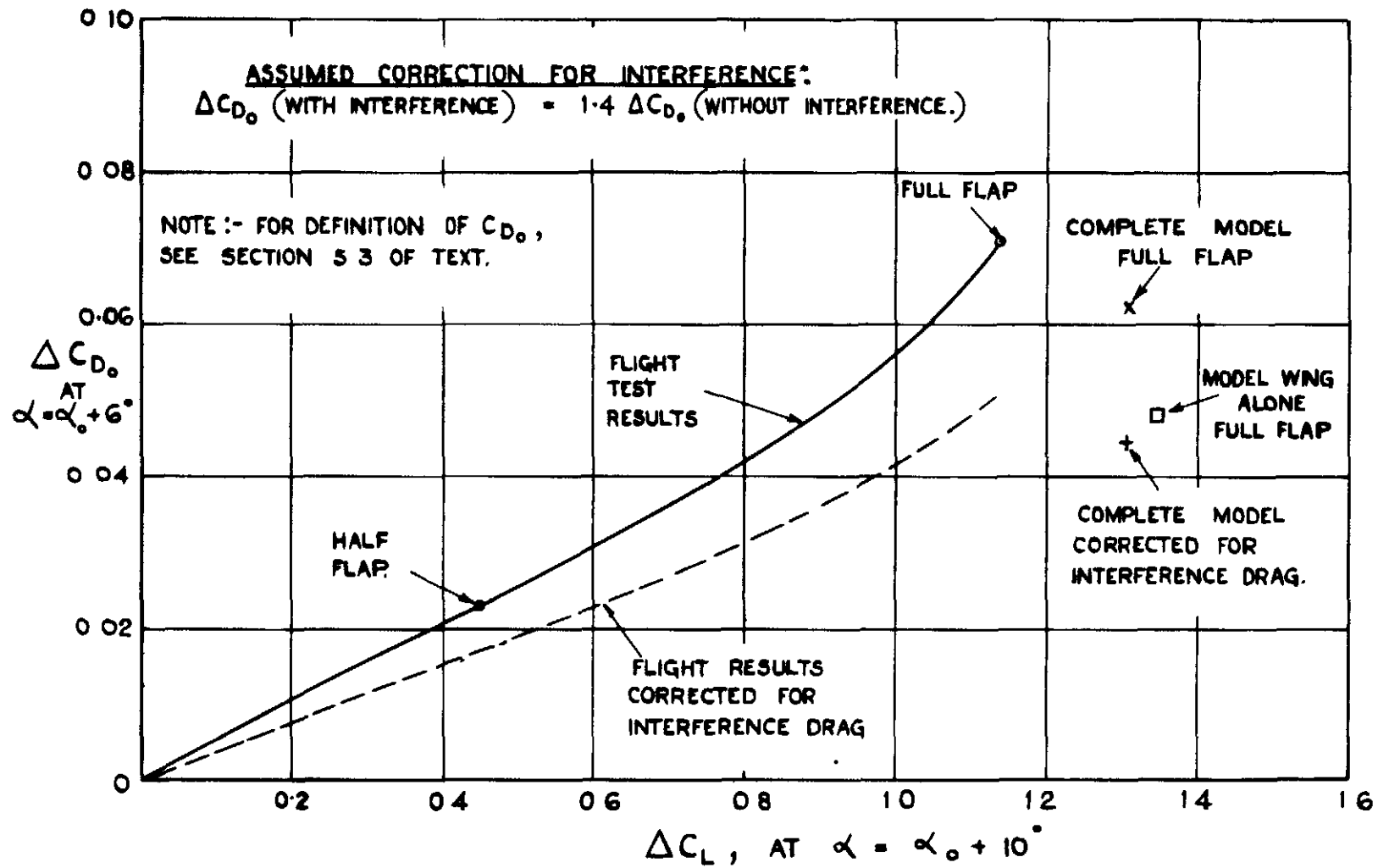


FIG. 15. LIFT AND PROFILE DRAG INCREMENTS DUE TO FLAPS.

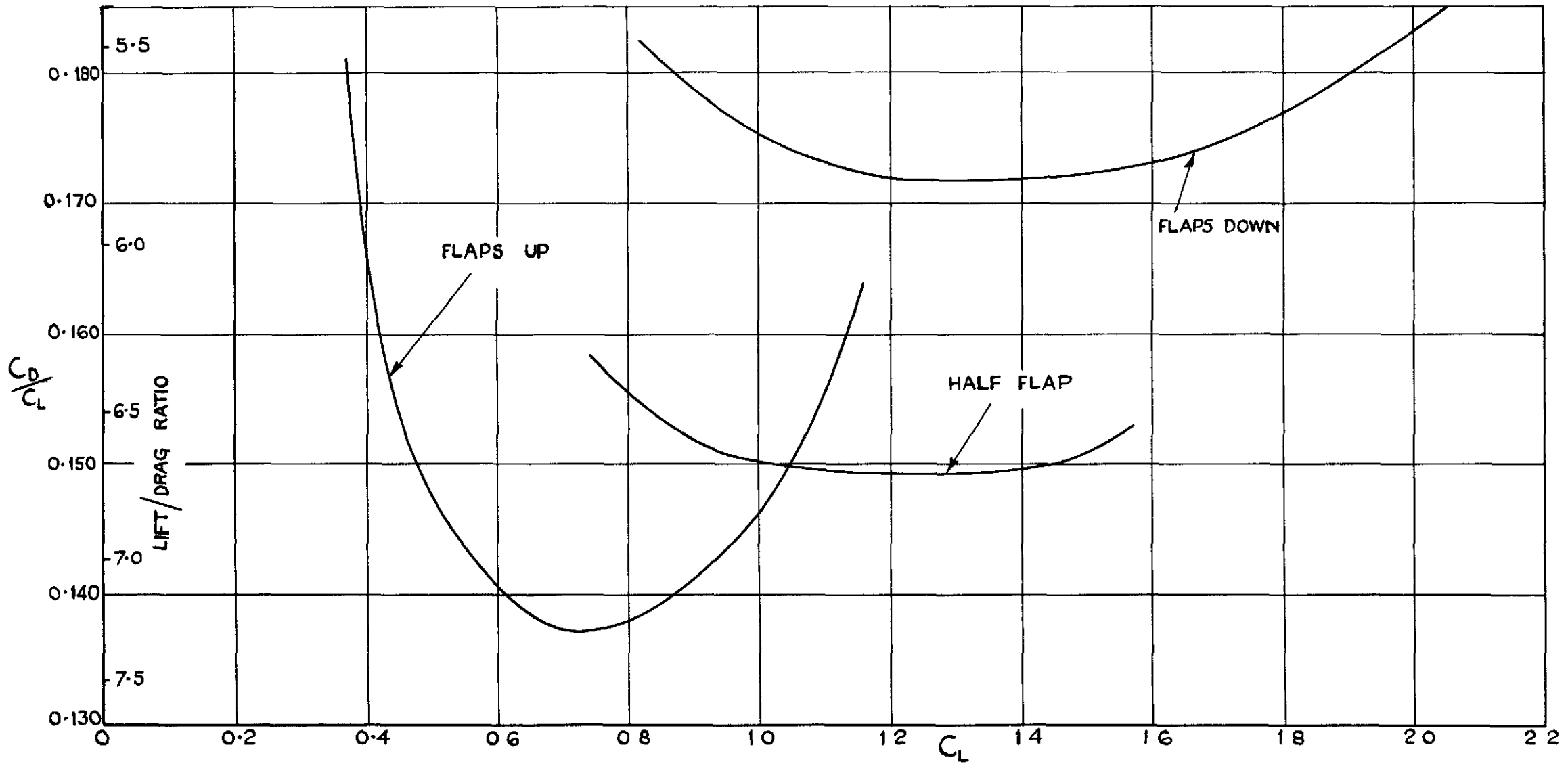


FIG.16. VARIATION OF C_D/C_L WITH LIFT COEFFICIENT.

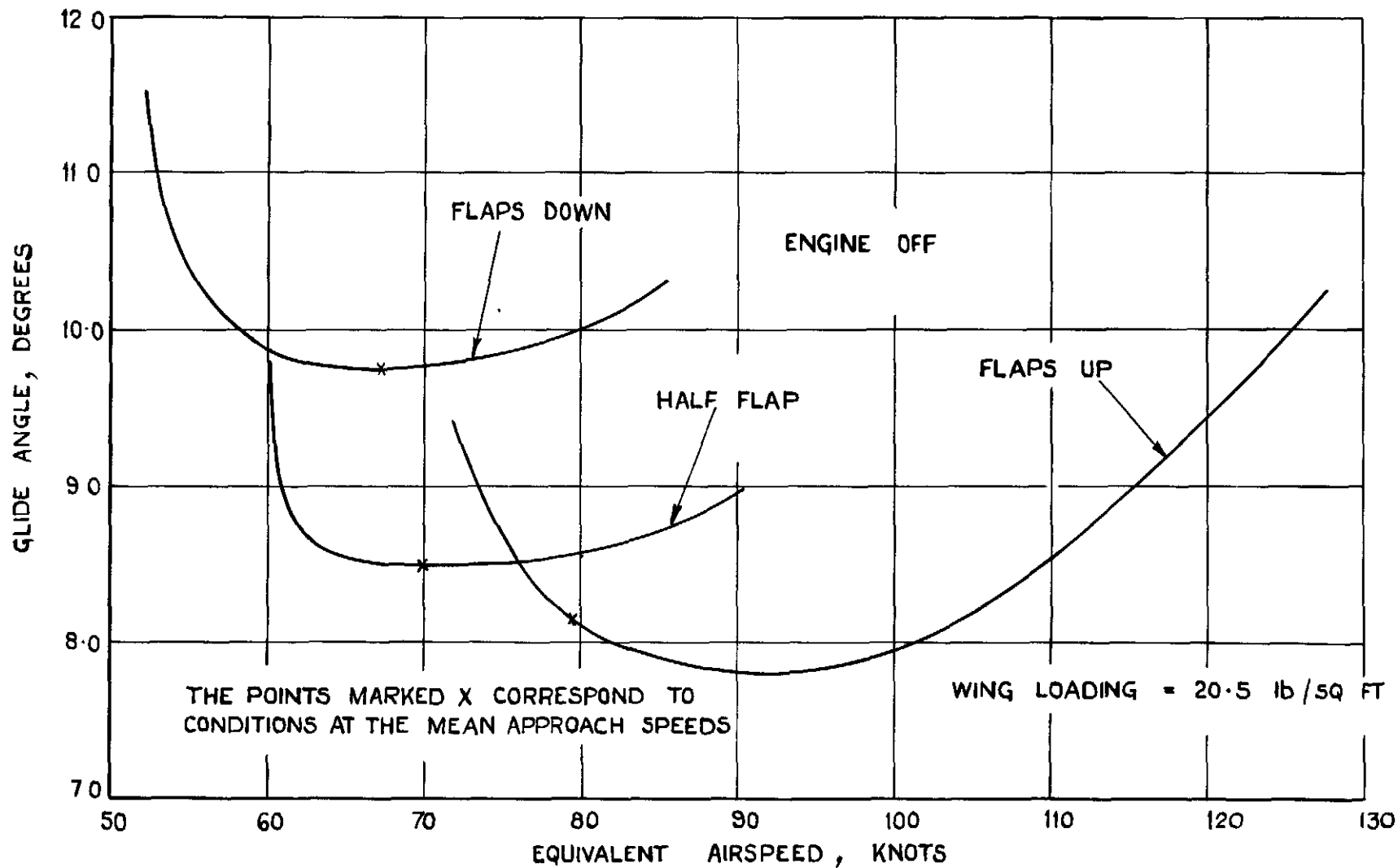


FIG.17. VARIATION OF ANGLE OF GLIDE WITH AIRSPEED.

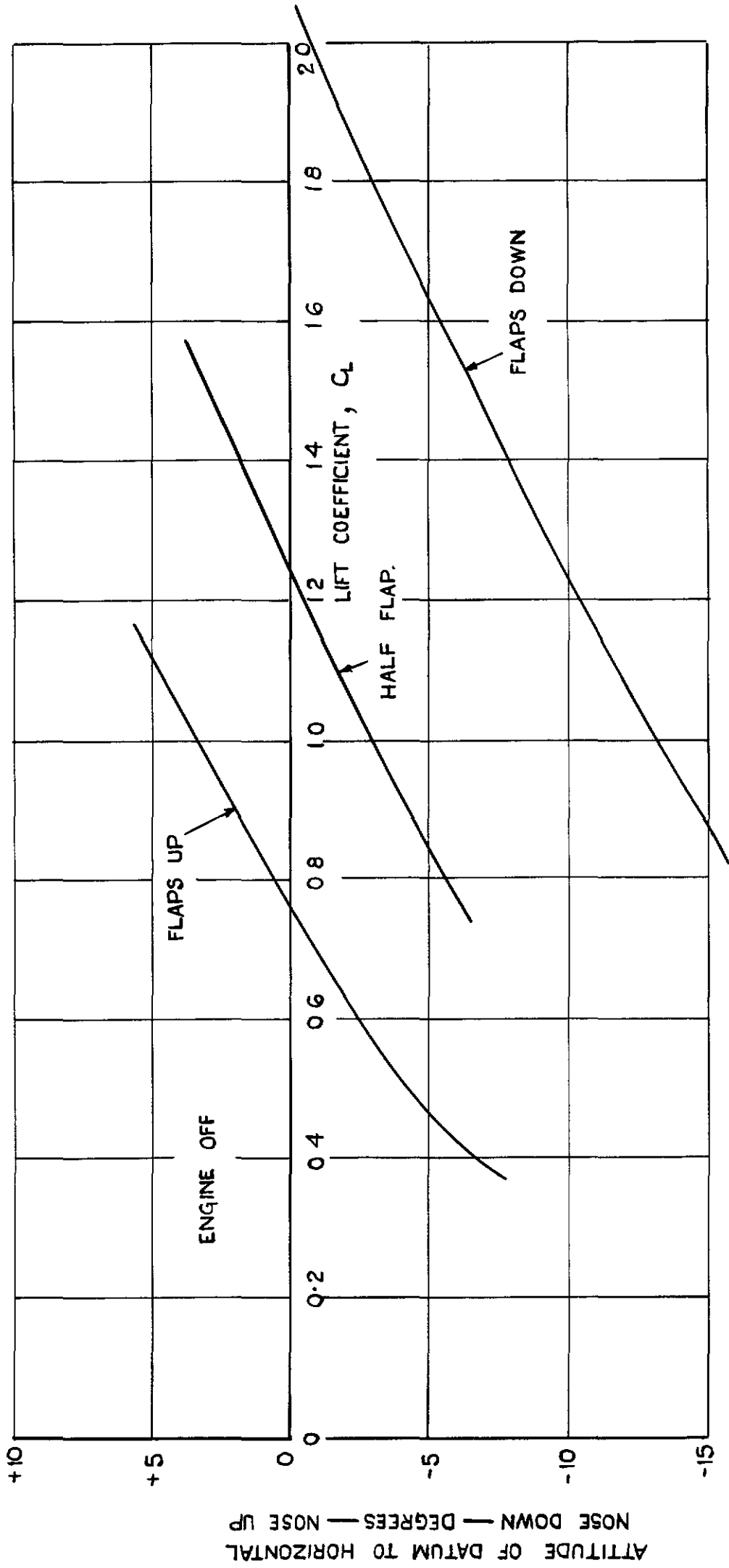


FIG. 18. VARIATION OF DATUM ATTITUDE WITH LIFT COEFFICIENT.

FIG. 19.

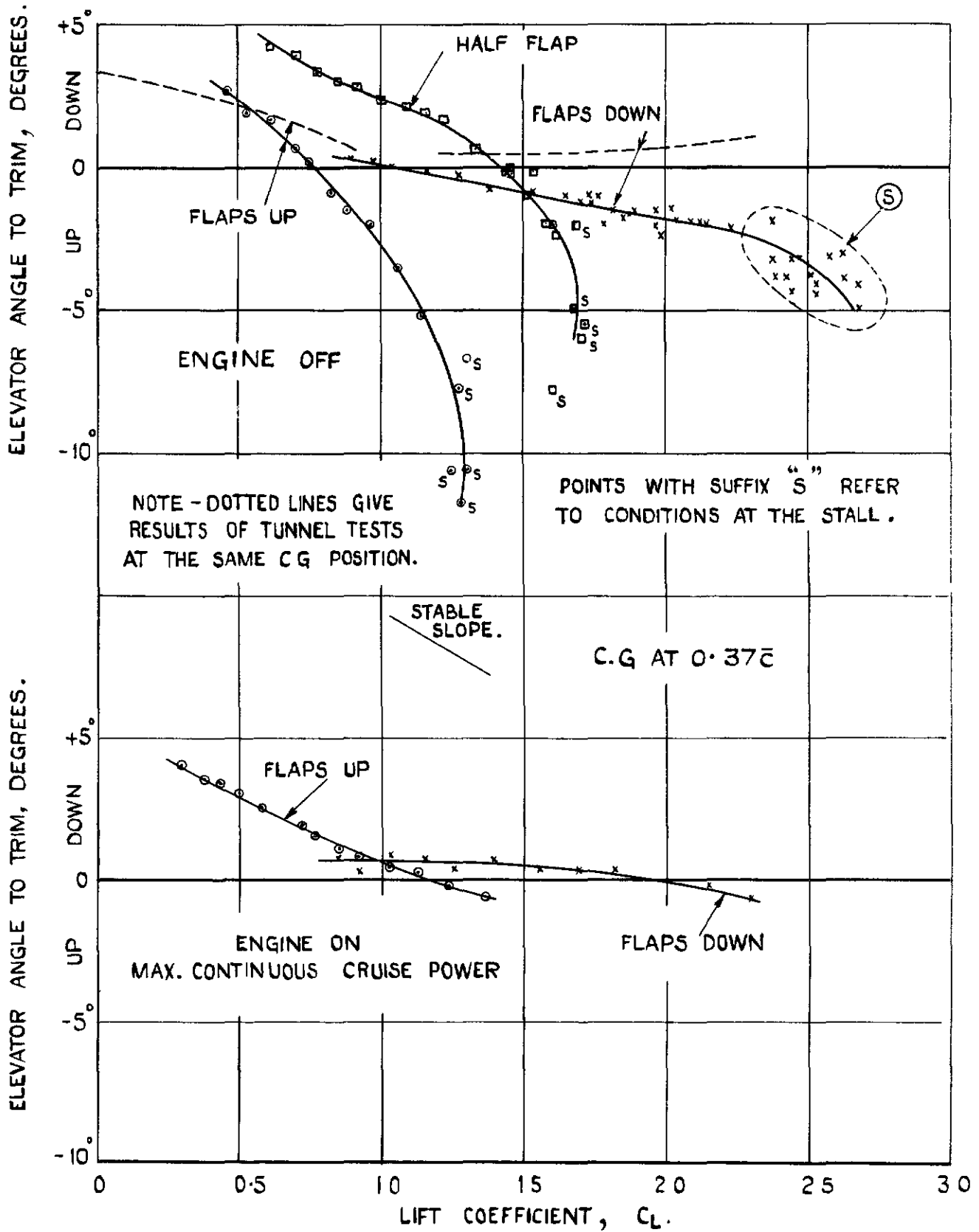


FIG. 19. VARIATION OF ELEVATOR ANGLE TO TRIM WITH LIFT COEFFICIENT.

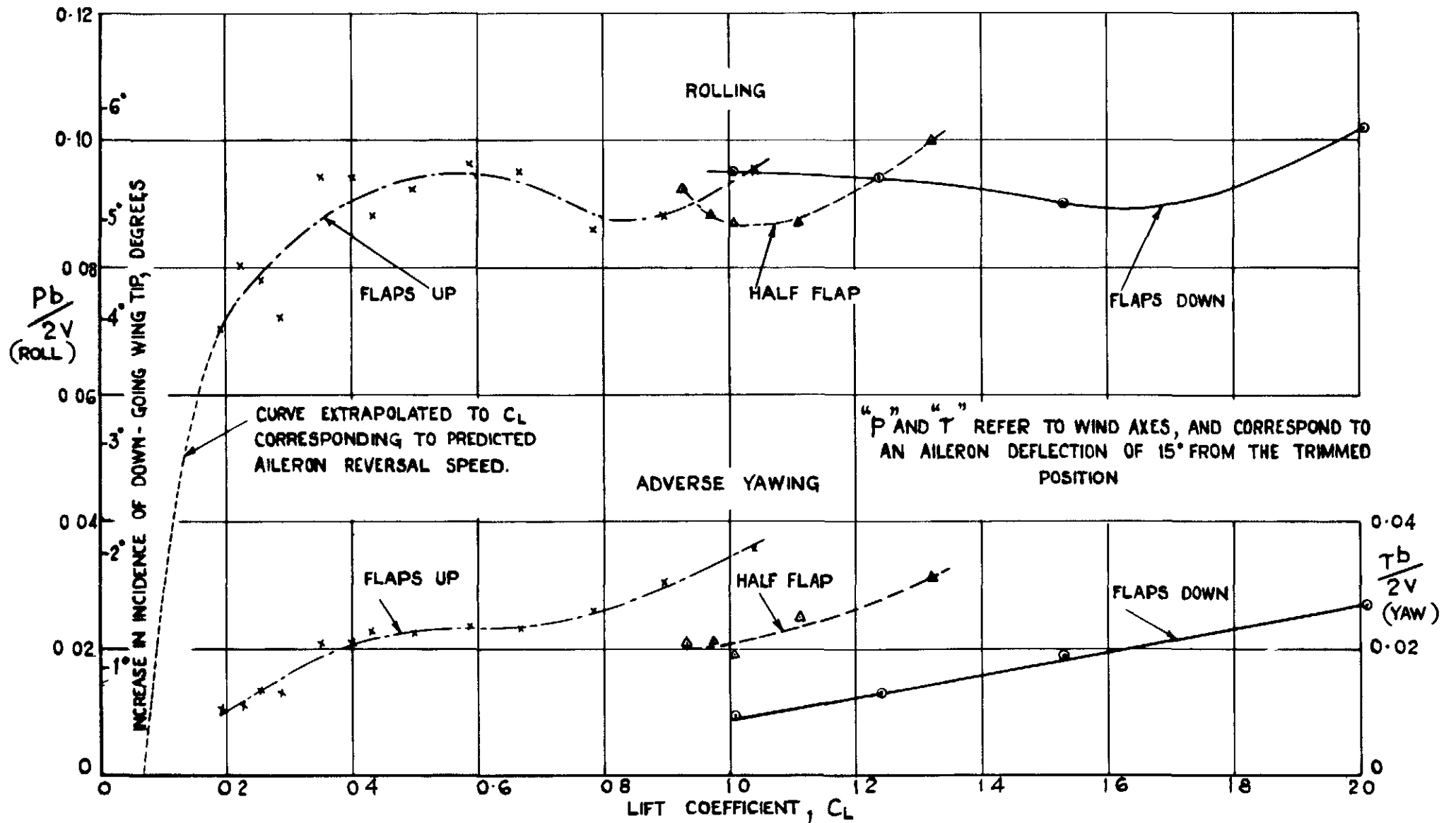


FIG. 20. VARIATION OF $\frac{pb}{2V}$, $\frac{\tau_b}{2V}$ WITH LIFT COEFFICIENT.

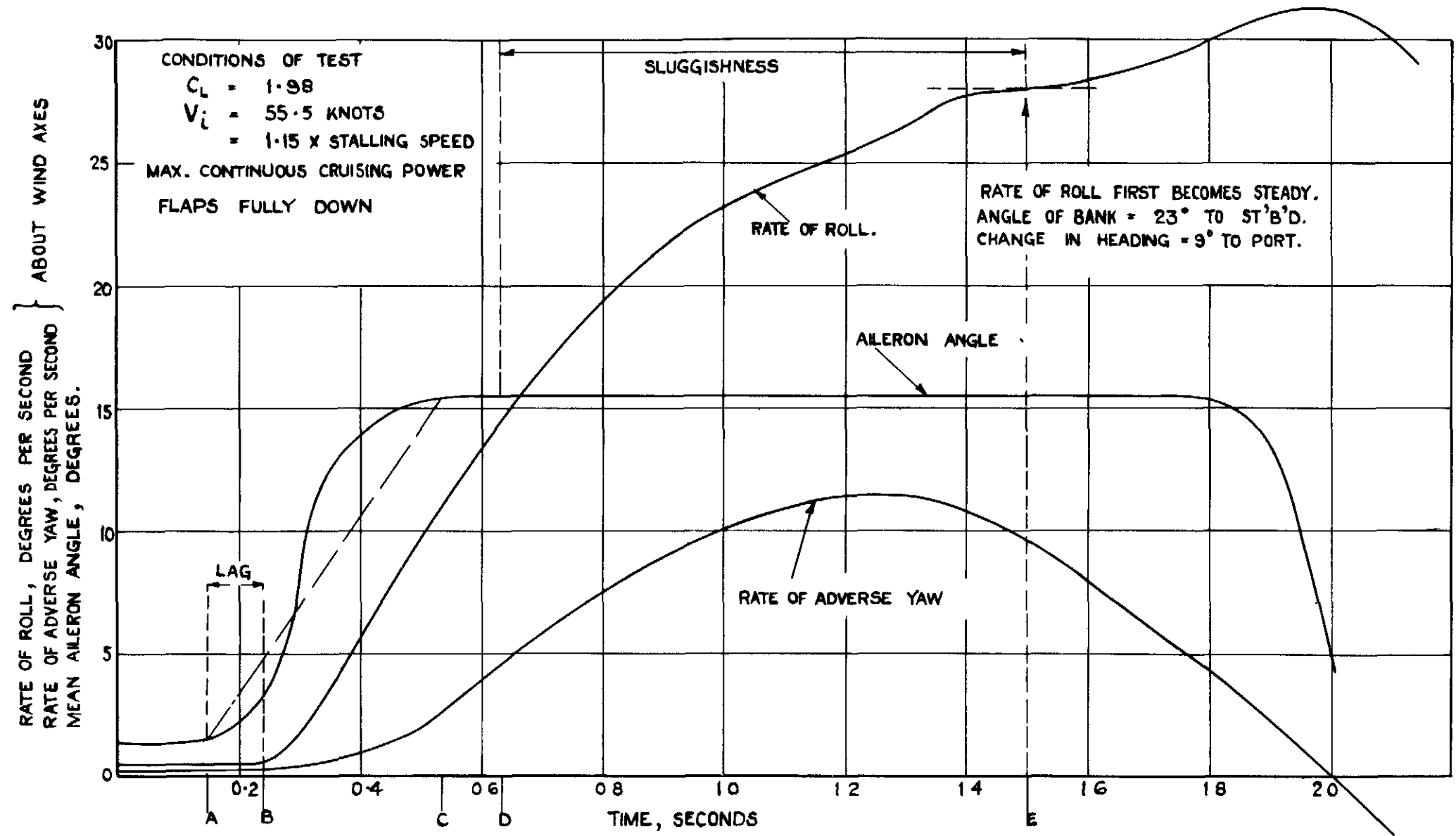


FIG. 21. TIME HISTORY OF TYPICAL RUDDER-FIXED AILERON ROLL, FLAPS DOWN.

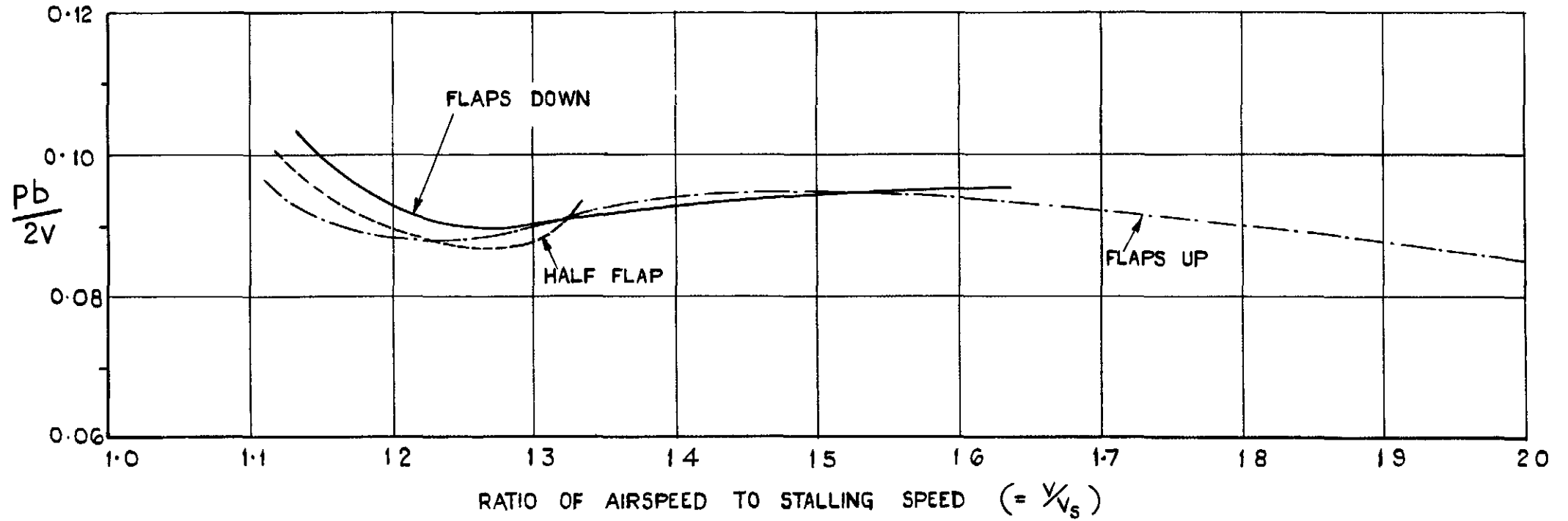
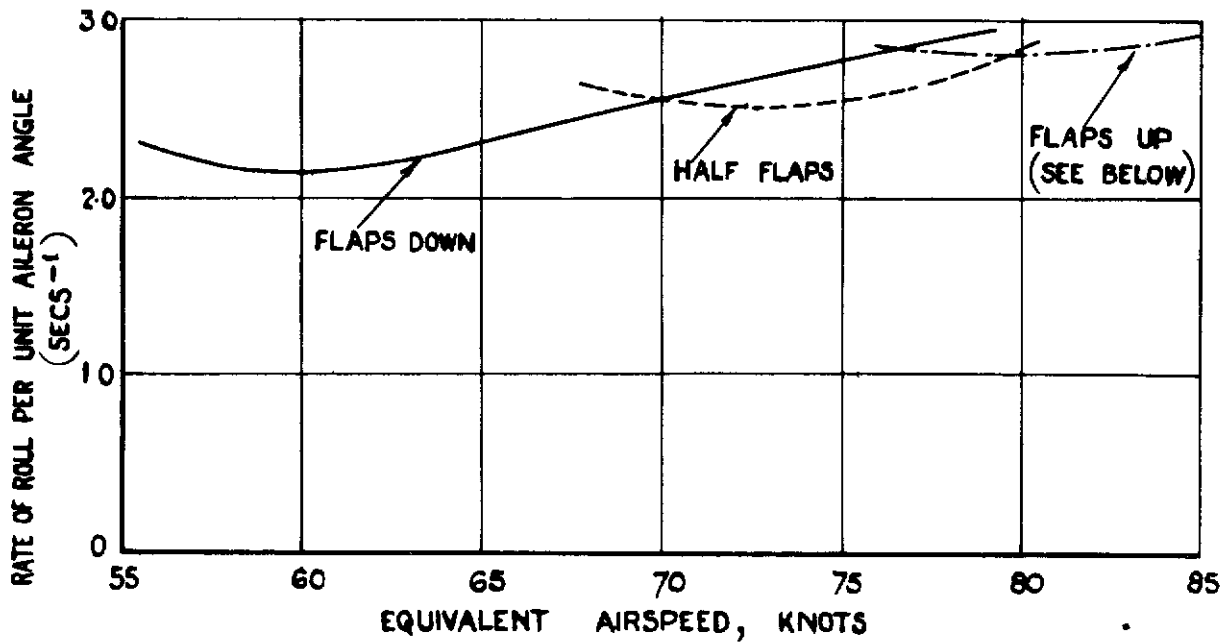


FIG. 22. VARIATION OF $\frac{pb}{2V}$ WITH SPEED MARGIN OVER THE STALL.

FIG. 23.



STANDARD SEA LEVEL CONDITIONS.

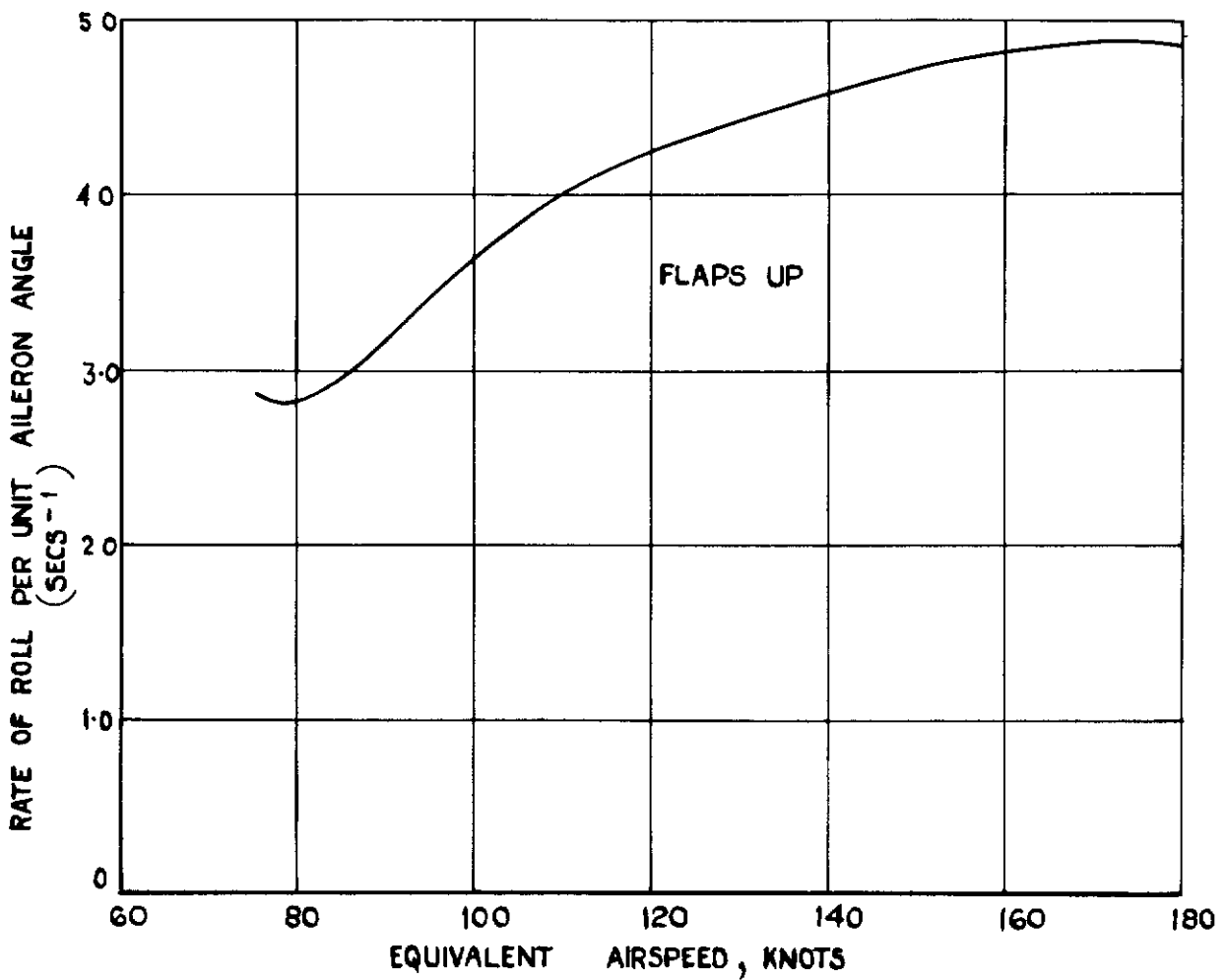


FIG. 23. VARIATION OF AILERON POWER WITH AIRSPEED.

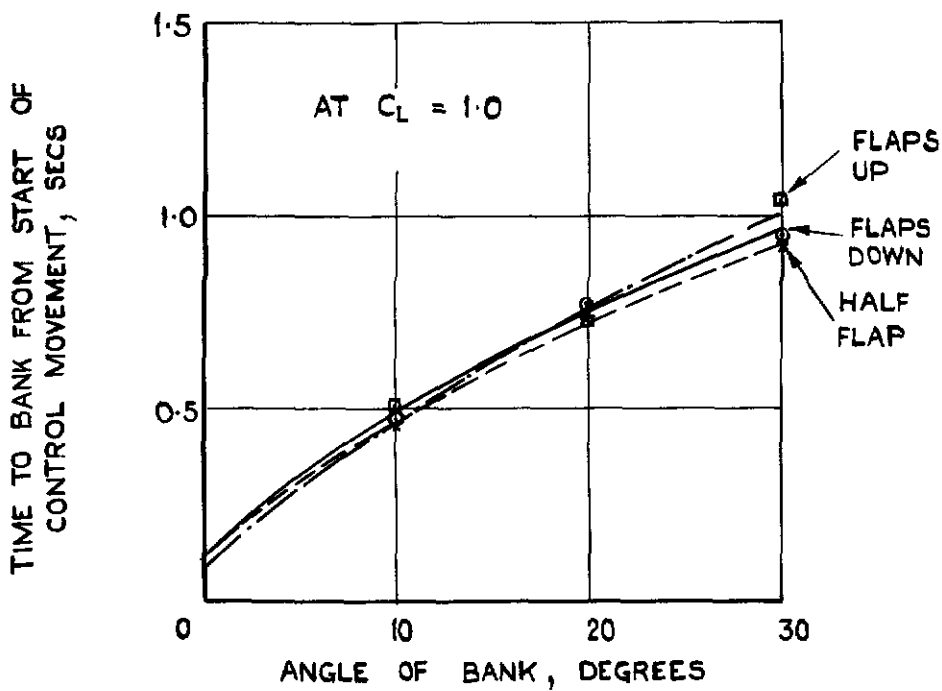
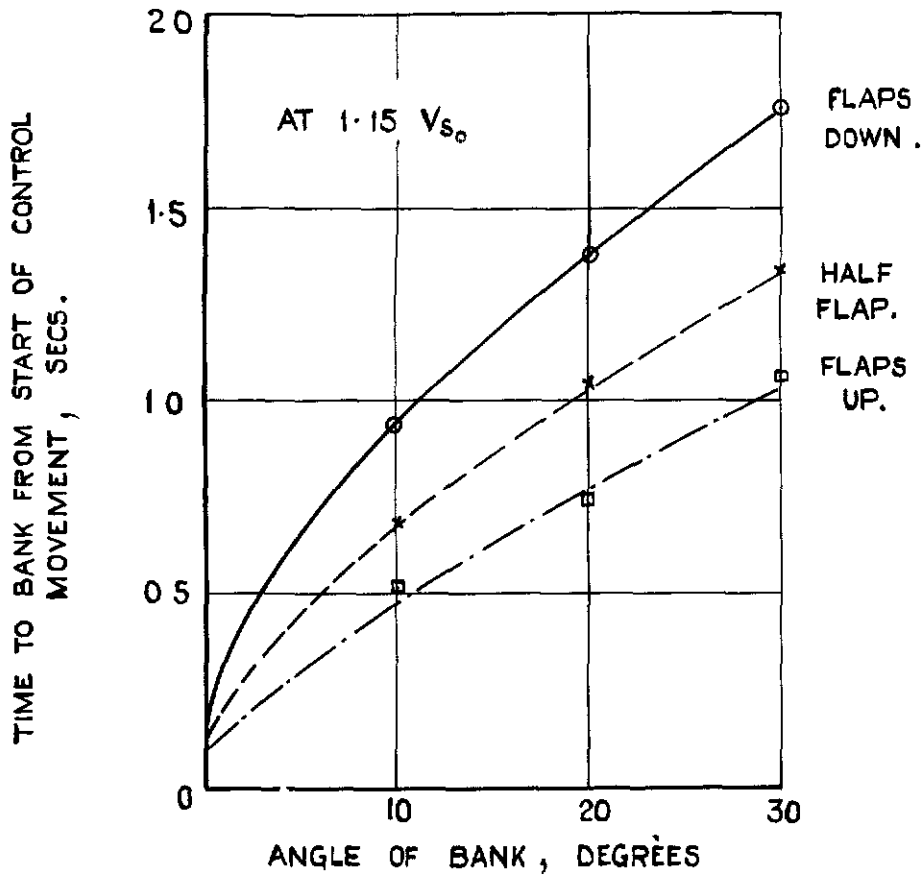


FIG. 24. TIME TO APPLY A GIVEN ANGLE OF BANK.

FIG. 25.

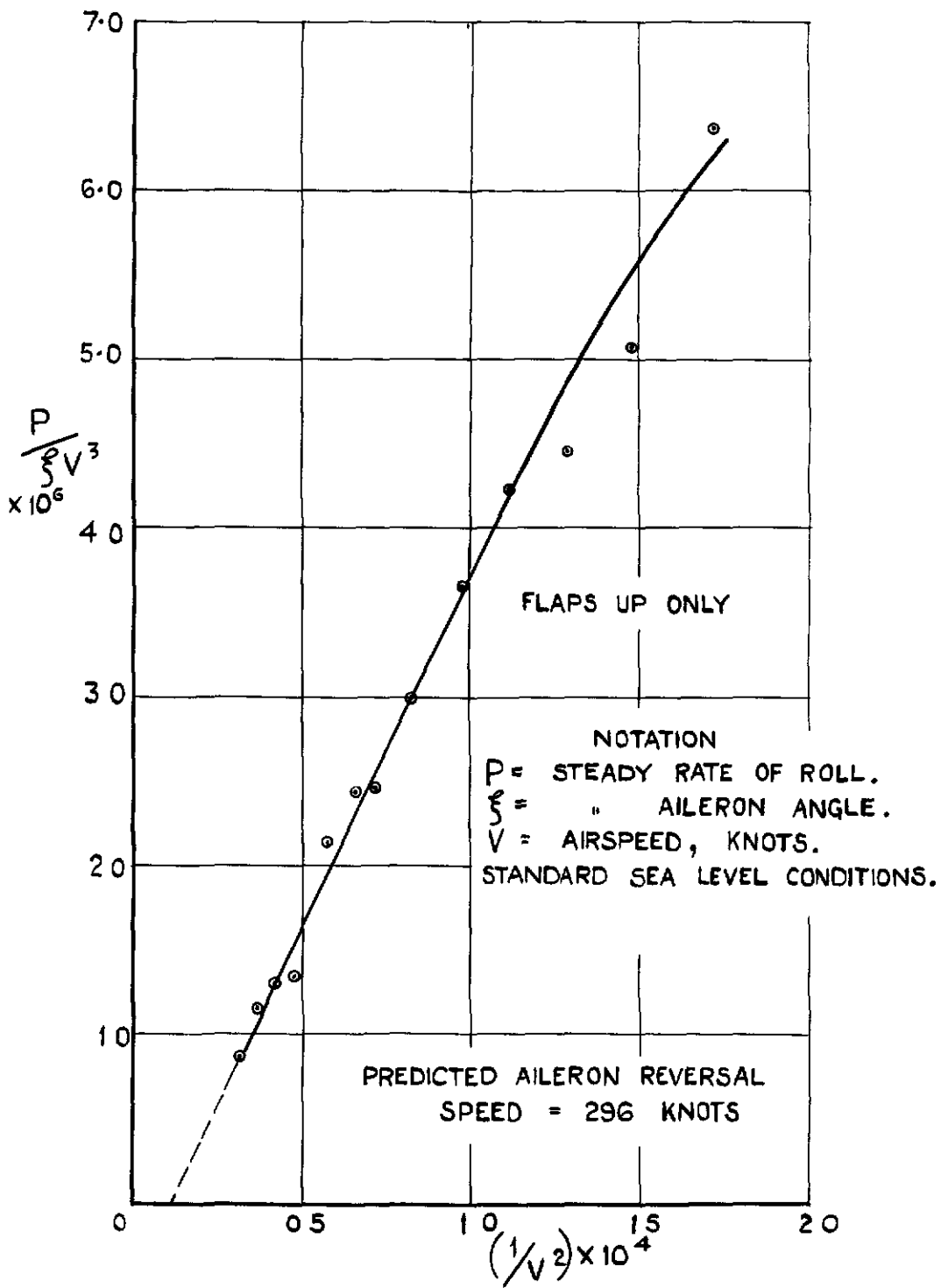


FIG. 25. PREDICTION OF AILERON REVERSAL SPEED.

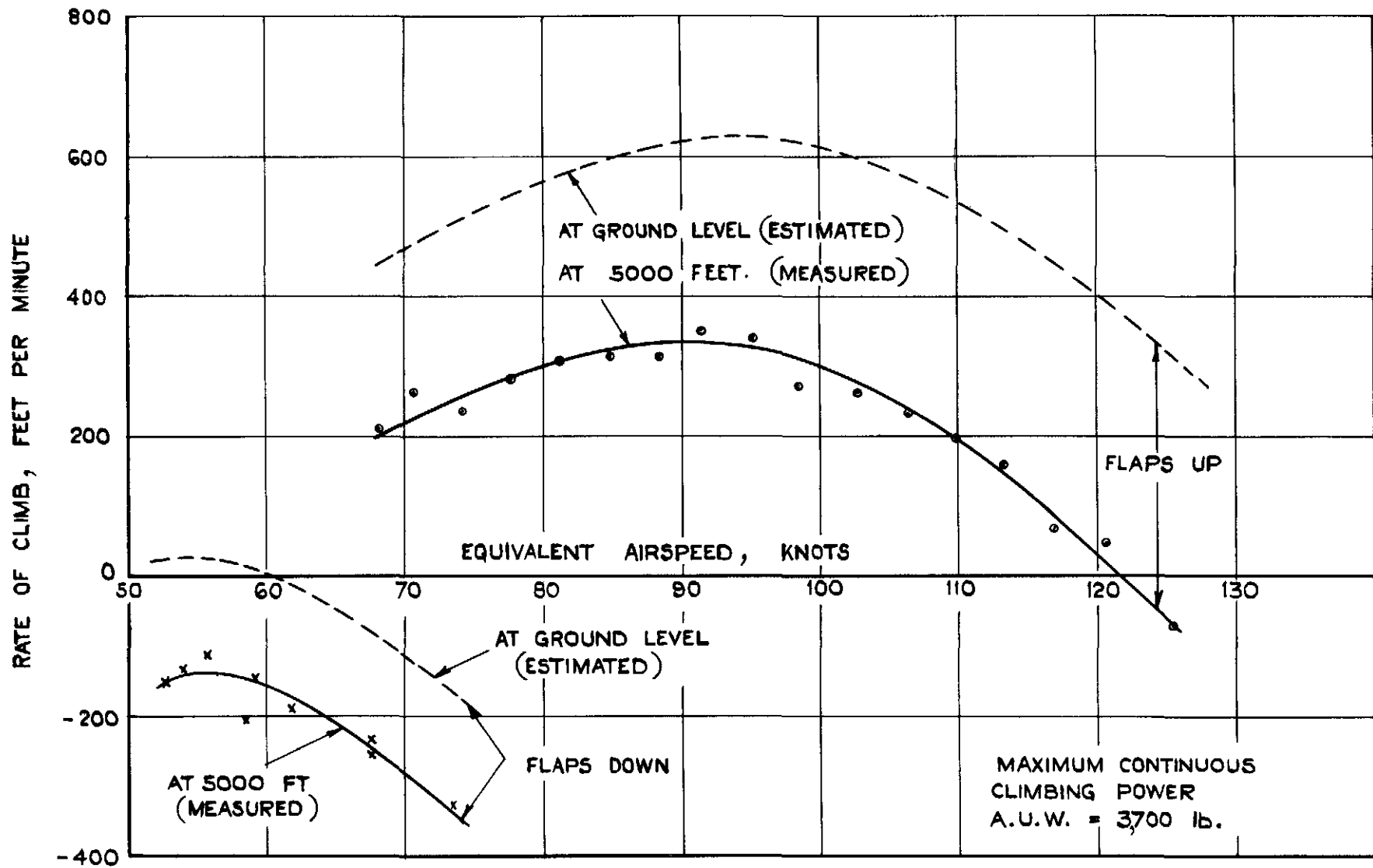


FIG. 26. CLIMB PERFORMANCE AT GROUND LEVEL & 5000 FT.

PUBLISHED BY HIS MAJESTY'S STATIONERY OFFICE

To be purchased from

York House, Kingsway, LONDON, W C 2, 429 Oxford Street, LONDON, W 1,
P O BOX 569, LONDON, S E 1,

13a Castle Street, EDINBURGH, 2		1 St Andrew's Crescent, CARDIFF
39 King Street, MANCHESTER, 2		1 Tower Lane, BRISTOL, 1
2 Edmund Street, BIRMINGHAM, 3		80 Chichester Street, BELFAST,

or from any Bookseller

1952

Price 10s. 6d. net

PRINTED IN GREAT BRITAIN